npj | 2d materials and applications

Review article

Published in partnership with FCT NOVA with the support of E-MRS

https://doi.org/10.1038/s41699-024-00462-z

Graphene oxide-based membranes for water desalination and purification

Saurabh Kr Tiwary [1,2], Maninderjeet Singh [1,2], Shubham Vasant Chavan [1] & Alamgir Karim [1]

Millions of people across the globe are severely afflicted because of water potability issues, and to proffer a solution to this crisis, efficient and cost-effective desalination techniques are necessitated. Membranes, in particular Graphene-derived membranes, have emerged as a potential answer to this grave problem because of their tunable ionic and molecular sieving capability, thin structure, and customizable microstructure. Among graphene-derived membranes, Graphene Oxide membranes have been the most promising, given the replete presence of oxygen-containing functional groups on its surface. However, the prospects of commercial applicability of these membranes are currently plagued by uneven stacking, crossflow delamination, flawed pores, screening and pH effects, and horizontal defects in the membrane. In addition, due to the selectivity–permeability trade-off that commonly exists in all membranes, the separation efficiency is negatively influenced. This review, while studying these challenges, aims to outline the most recent ground-breaking developments in graphene-based membrane technology, encompassing their separation mechanism, selectivity, adjustable mechanical characteristics, and uses. Additionally, we have covered in detail how several process variables such as temperature, total oxygen concentration, and functional groups affect the effectiveness of membrane separation with the focal point tilted toward studying the currently used intercalation techniques and effective nanomaterial graphene oxide membranes for water desalination

Membrane-based technologies for applications in separations are to be reliable and game-changing in terms of energy efficiency when compared to thermal processes[1,2]. The current prevalent polymeric membranes experience poor selectivity, low fouling resistance, and low stability to abide heat or chemical lured decadence. poised Therefore, searching and exploring a novel material, with mended selectivity, permeability, resistance to fouling, and chemical stability concurrently, for membrane fabrication has been a consistent endeavor[3]. In the past decade, Graphene oxide membranes (GOms) constituting tunable microstructures and multifunctional reactive groups have attained enormous potential to demonstrate high water permeability, thus captivating significant scientific and technological interest[3,4] (Fig. 1). The water permeability in GO membrane is governed either via the oxidized zones that serve as spacers to administer sufficient interlayer distance to accept water molecules, or via pure graphitic zones by enabling practically unhindered flow[5].

Moreover, to further impact the graphene oxide membrane's selectivity and permeability, the interlayer d spacing of GOms can be adjusted by ensuring precise sieving[6] based on the feed molecular size[5,7]. Supplementary to this, GO membranes are mechanically reliable, inexpensive, and suitable for industrial-scale production[8,9], making them a perfect candidate for water desalination[3,10–18]. There are two categories of GOms that have attracted attention while acclaiming water selectivity and permeability: ultrathin nanoporous GOms (porous graphene)[19–26], and GOms with two-dimensional water channels in a stacked-layer form (including the intercalated GOms)[5,27–32]. The atomic thickness of nano-porous GOm is around one-third of a nanometer, that results in larger values of water permeability (6–66 L cm^{-2} MPa^{-1}) than in thin-film composite membranes (~0.24 L cm^{-2} MPa^{-1}) while accomplishing near complete salt rejection (~100%)[33]. However, consistently creating defect-free sub-nanometer holes (radius ~0.45 nm) on a single layer of graphene is challenging and faces scalability issues. Therefore, the application of nano porous graphene for desalination is currently an ongoing research work[34–36]. Although there has been extensive research going on two-dimensional GOms (both chemically treated and physically intercalated)[37]. But these 2D membranes often contain microporous defects that emerge from the improper stacking of graphene oxide (GO) laminates, also known as framework defects[38,39]. In a recent study by Zhang et al., these microporous defects were path blockers in the water-solute selectivity of GO membranes[39]. Their impact can be

[1]Department of Chemical and Biomolecular Engineering, University of Houston, Houston, TX 77204, USA. [2]These authors contributed equally: Saurabh Kr Tiwary, Maninderjeet Singh. e-mail: akarim3@central.uh.edu

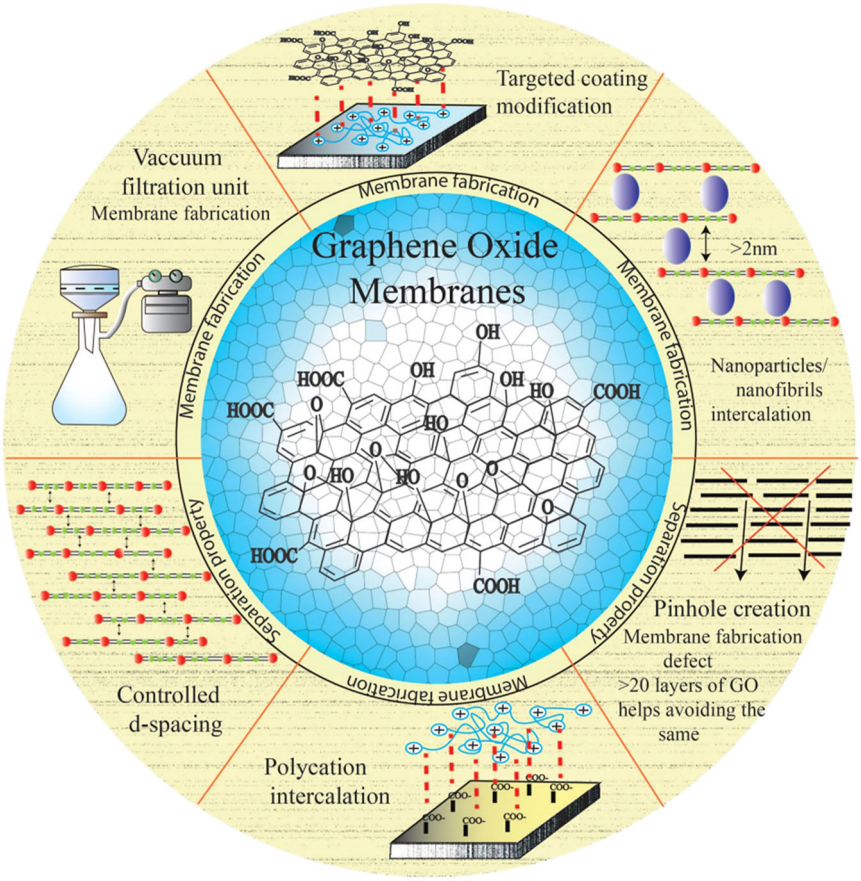

Fig. 1 | Graphene oxide membrane: from fabrication to separation properties. Description—mechanism of graphene oxide membrane-based separation.

estimated by the degree to which they are filled; particularly, more selective membranes are produced by GO membrane microstructures with fewer or smaller spaces. Another challenging aspect with GOm is the framework's stability; GO nanosheets get delaminated, or the tiny gaps get compacted under normal working conditions[40].

Therefore, substantial efforts are required in this field to develop membranes for desalination applications that are both robust and scalable. In the context of desalination, unfortunately, the majority of graphene oxide (GO) membranes examined to date have been evaluated with feed solutions containing less than 0.1 wt% NaCl and exposed to a pressure of 0.5 MPa. Additionally, most of these systems employ laboratory-use dead-end flow unit, which operate differently from industrially acceptable cross-flow units[41]. Moreover, these low salt concentrations are present in tap water, certain industrial processes, agricultural operations, and similar contexts. Therefore, innovative membranes intended for water desalination need to exhibit robustness to endure crossflow velocities, preventing delamination, especially in industrial saline wastewater (~0.1M)[42].

In summary, up to date none of the reviews discuss in detail the role of GOms, specifically for water desalination, while demonstrating the gravity of GOms separation mechanism[43] and selectivity, the effect of different process parameters (total oxygen concentration, functional group, and temperature), different ways for tuning the mechanical properties of GOms while discussing the nanomaterial GOms simultaneously. Thus, our motive in this review is to delve deeper into GO membranes and discuss their recent achievements, especially in the field of water desalination while highlighting the areas for further improvement. Here, the discussion, delves into recently developed GOms that effectively challenge the tradeoff between permeability and selectivity. These innovative membranes address this rule through distinct approaches. One such approach, suggested by multiple researchers, involves bolstering the stability of GO membranes in aqueous environments through cross-linking agents containing metallic cations, such as Al^{3+}[41,44]. However, a notable challenge accompanying this method pertains to its susceptibility when subjected to both acidic and alkaline conditions[45]. Thus, in the subsequent section, we have discussed the feasible intercalants and the role of nanomaterials that can lead the way toward ultra-high separation efficiency membranes[46,47]. This will serve as a guiding torch for the upcoming researchers in this field to develop the next generation of GO membranes.

GOms separation mechanism and selectivity

GO nanosheet is a 2D nanomaterial[35,48] whose thickness is of the order of one atomic thickness with a limited percentage of holes and oxidized areas over its surface[13,49] The formation of a GO membrane, possessing appreciable mechanical strength, necessitates the piling up of several units of nanosheets together[46]. In an aqueous environment, molecules or ions can travel through the GO membrane. This ability to transport water is attributable to (1) the existing gaps between the non-interlocked adjacent GO sheet's edges, (2) the interlayer nanocapillary network generated from linked interlayer spaces, gaps between the non-interlocked-adjacent GO sheet's edges, and (3) minute faults (holes/cracks) existence in the GO sheet[46]. The GO membrane's ability to conduct separation depends on its molecular or ionic properties, e.g., size, charge, and interactions with the membrane. The extent to which the gaps between adjacent GO sheets influence the separation can be changed if the membrane's thickness and the sheet's size are adjusted. One way for the membrane to efficiently reach appreciable levels of separation might be to modify the gap between the GO membrane's multiple layers, which can be done by changing the water pH, intercalant agent, and the dimension of GO sheet[47].

Nanochannels' exhibiting the so-called "size exclusion effect" within the GO membrane structure might filter large organic molecules as shown in Fig. 2a. To precisely exclude ionic and giant molecules based on their size, Mi et al. suggested manipulating the GO spacing of the nano-channels[50]. Consequently, with the introduction of certain nanofillers[51] and cross-linkers[52] between the sheets of GO, it is possible to develop membranes for desalination

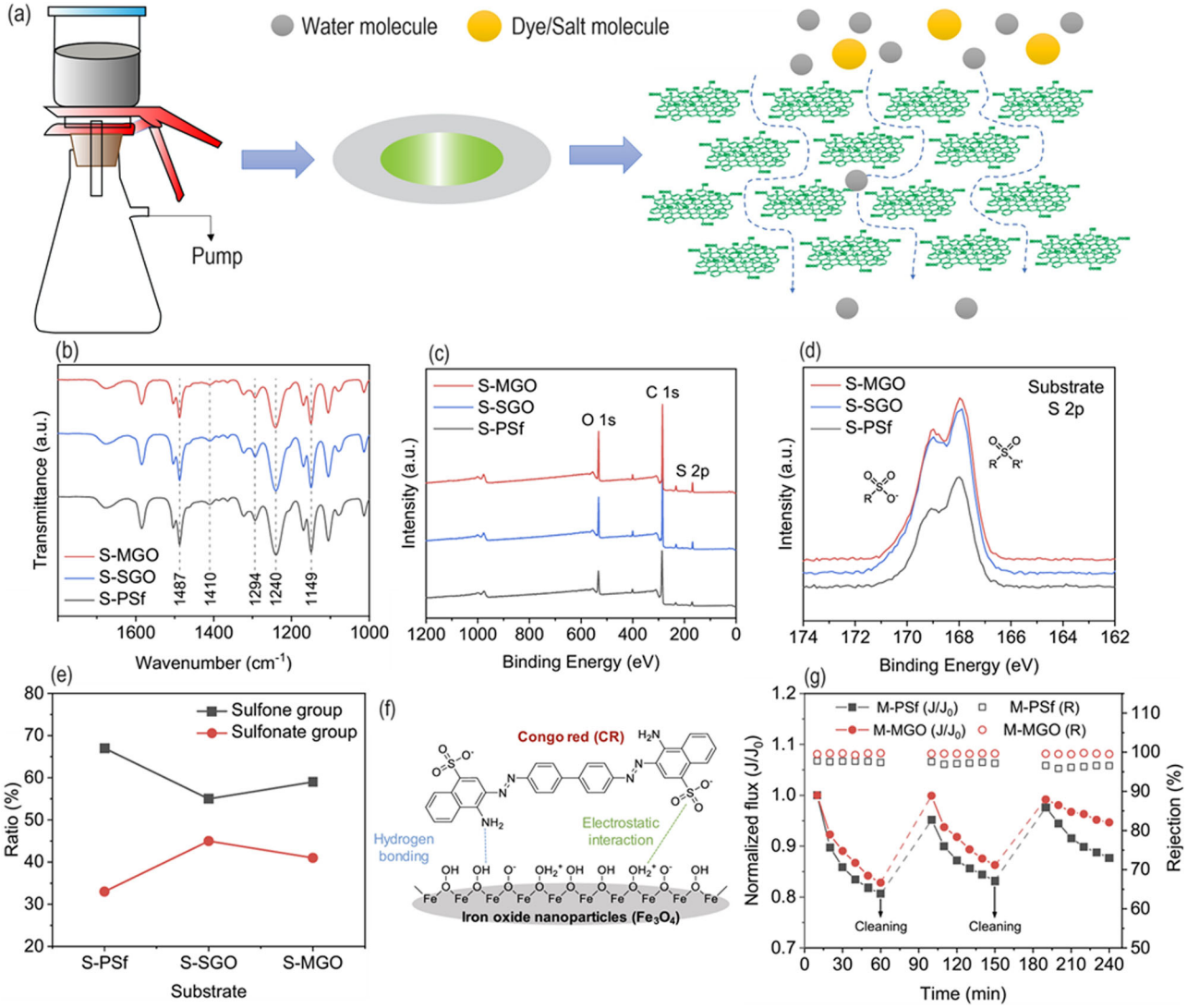

Fig. 2 | Illustration of water transport through GO membranes and their characterization. a Graphene oxide membrane fabrication and permeation characteristic in 2D graphene galleries. **b** ATR FTIR Spectra, (**c**) XPS Spectra, (**d**) High-resolution S 2p XPS spectra, (**e**) the ratio differences between sulfone and sulfonate groups based on the substrate, (**f**)The figure depicts the adsorption mechanism that has been proposed for CR dye on iron-oxide nanoparticle, (**g**) On the two vertical axes, the normalized flux and percentage of rejection are compared for M-Psf and M-MGO membranes, where CR is the foulant, as a function of time over three regeneration cycles[69]. Reprinted under terms of the Creative Commons license from ref. 69. Copyright 2022 Elsevier. Description—analyzing structural characterization and rejection percentages of graphene oxide membrane in different conditions.

applications with precise inter-layer spacing[53]. In addition to the size-sieving effect, there is a possibility that charged ions and tiny molecules might be rejected by the Donnan exclusion effect (unequal distribution of permeant ions) in GO membranes[54,55]. GO is negatively charged throughout an extensive pH range because of the deprotonation of carboxyl groups at the margins of GO nanosheets. This makes it possible for the pure GO membranes to have strong rejections for organic molecules or divalent ions that are negatively charged[13,56]. The inherent negatively charged properties of GO membranes are not set in stone and can undergo alterations. Wang et al. conducted recent research involving the synthesis of three distinct GO membranes: GO-1, GO-2, and GO-3. Interestingly, at lower transmembrane pressures of 10 bar, the first two membranes displayed negative rejections towards divalent salts. However, when faced with a monovalent salt like NaCl, all the membranes exhibited negative rejections due to Donnan equilibrium. This behavior, which emerges as a consequence of interactions between monovalent and multivalent salts, as well as charged organic species with significant sizes, underscores the complexity observed in NF membranes[57].

The ionic concentrations near the membrane surface are not the same as those found in the bulk solution, as per Donnan exclusion [58]. When compared to the bulk solution, the concentration of counterions is larger at the membrane surface. The concentration of co-ions, or ions with the same charge as the membrane, is lower at the membrane surface. Water can travel through the membrane when it is under external pressure, but co-ions cannot because of the Donnan potential[59]. Counterions are also rejected at the same time due to electroneutrality criteria. The rejection (R) of various salts is given by the following equation according to Donnan's theory[57]:

$$R = 1 - \frac{c_i^m}{c_i} = 1 - \left(\frac{|z_i| c_i}{c_x^m + |z_i| c_i^m} \right)^{\left| \frac{z_i}{z_j} \right|} \quad (1)$$

Here,

z_i and z_j denote the valency of co-ions and counterions.

c_i and c_i^m denote co-ion's concentrations in bulk and on the membrane surface.

c_i^m denotes the membrane charge concentration.

i denotes the co-ions. j denotes the counter-ions.

Strong adsorption caused by the varied interactions of ions over various locations on GO sheets also allows the removal of some smaller hydrate ions with excellent selectivity[60]. This was driven by GO membranes' ability to completely inhibit coordination contacts between transition metal cations and the oxygen-containing functional groups[61]. Similar to this, the rate of penetration for alkaline earth and alkaline cations are lowered because there exists contact with GO's sp^2 cluster[62]. In the work by Han et al., a vacuum-assisted filtration setup was utilized to create ultrathin GO membranes for water purification that ranged in thickness from 22–53 nm on porous polymer substrates. The resulting ultrathin NF membranes exhibit a 99% retention rate for organic dyes and a water permeance of 21.8 L m^{-2} h^{-1} bar^{-1}, which is on the higher side[63]. An ultrathin GO layer for NF can be constructed by utilizing a minute amount of GO.

Due to the minimal material usage resulting in an economical approach, manufacturing such a membrane becomes viable. This is coupled with the application of a phase inversion technique to facilitate the production of magnetite-decorated graphene oxide (MGO) and sulfonated graphene oxide (SGO). The insertion of these materials into the substrate's polymer matrix was carried out individually. Notably, the substrates enhanced with these additives exhibited improved hydrophilicity, surface roughness, porosity, and pure water permeance in comparison to the pristine substrate. In a study, Kieu et al. demonstrated that the surface roughness of GOMs can impede the natural spreading of water molecules and diminish the hydrophilicity of the GO surface[64]. The presence of surface roughness in GOMs can create obstacles and irregularities that water molecules need to navigate, slowing down their movement and reducing the contact area between the water molecules and the GO surface. This can lead to reduced wetting and hindered water permeation through the membrane. The reduced spreading and diminished hydrophilicity caused by surface roughness can affect the desalination performance of GOMs. To mitigate the negative effects of surface roughness, various strategies can be employed, such as surface modification or optimization of the synthesis process. With the objective of smoothing the surface and augmenting the hydrophilicity of GOMs to enhance desalination performance, these approaches come into play. As a result of the active layer's loose structure, the MGO NP-embedded TFC membrane (M-MGO) showcased notable salt permeation and water permeance[65].

In Fig. 2b, the authors have shown the results derived from ATR-FTIR for the S-PSf, S-SGO, and S-MGO substrates. Figure 2c depicts the XPS spectra used to analyze a substrate's chemical compositions of S-PSf, S-SGO, and S-MGO. In Fig. 2d, the authors depicted a high-resolution XPS spectrum of S 2p, while in Fig. 2e, a graph between the ratio of sulfone to sulfonate groups and the substrate was plotted. Kang et al. carried out three regeneration cycles to collectively examine the antifouling effectiveness and regeneration capacities of two membranes, M-PSf and M-MGO. Figure 2g shows the membranes' CR rejection and normalized flux, which is time-dependent and denoted by J/J_0. Each cycle involved permeating a 30 milligram per liter CR solution at 5 bars for 1 h, followed by a half-hour membrane washing with NaOH 0.1 M. Due to the dye foulant, the permeate flux gradually dropped; nevertheless, following chemical cleaning, the flux was restored. The authors have also explained the adsorption of negatively charged dyes on ferric oxide through a number of different mechanisms[66–68]. There are two key factors (Fig. 2f) that contribute to the CR dye's adsorptive process on Fe_3O_4. The first factor is hydrogen bonding, and this explanation is related to the functional groups in Fe_3O_4 that carry the oxygen atom, i.e., the hydroxyl group. The second factor is the attraction between the negative charge on the $-SO_3$ group of CR molecules and the positive charge on the $-OH^{2+}$ group of Fe_3O_4. Ferric oxide is a capable enough compound to adsorb the CR dye, and this is because of the negative interactions occurring between the free-CR dye and the benzene rings of the already-adsorbed CR dye on Fe_3O_4[69].

Also, according to specific investigations, carbon nanotubes and nanoparticles can be added to GO laminates to create nano-channels and increase gaps for quick water movement without reducing rejections to organic solutes[70–74]. These fillers could also be eliminated to lower the mass transport resistance further. To increase membrane permeability, Huang et al. presented a new nano-strand-channeled GO membrane[75] employing copper hydroxide nano strands as the sacrificial template. To put it another way, firstly, the insertion of nano-strands of copper hydroxide was done inside the GO membranes, and then they were dispersed so that larger channels for water flow could be created. Owing to this, the water permeance increased by ten-fold without compromising on the rejection. Consequently, the key lies in microstructure adjustments, offering a pathway for the development of GO membranes with heightened water permeability, potentially resulting in significantly improved membrane properties. Moreover, an additional avenue for enhancement involves the application of an external electric field onto the GOms, opposing the water flow direction, which has been observed to elevate the solute rejection capability of GOms[76,77]. This method is known as electric-field-induced ionic sieving and has been shown to be effective in miniaturized water desalination. A study conducted by ref. 77 in 2020, which employs MD simulations to determine the performance of bilayer GOms which are ionized for the desalination of seawater, supports the idea that when external electric field is applied in a direction opposite to the flow of water, the GOms' salt rejection ability can be elevated. Dahanayaka et al.[77] concluded in their research that their membrane possessed high water permeability and salt rejection. Given the presence of an external electric field, an electric potential is induced across the ends of the membrane that directly governs how ions and water molecules transport through the membrane. It is worth noting that if the directions of the applied electric field and flow of water oppose one another, an increment in the membrane's solute rejection is observed, given the induction of a repulsive force between the membrane and ions. It is this repulsion that leads to an increment in solute rejection. Supplementary to this, the mobility and orientation of water molecules are a function of the applied electric field, and this is an additional reason why we observe an increase in the extent of water that transports through the membrane[77,78]. Therefore, applying an external electric field in the direction opposite to the flow of water can improve the performance of GOms for seawater desalination. However, the research paper by ref. 77 focuses on the effect of ionisation on the seawater desalination performance of a bilayer ionised graphene oxide (IGO) membrane using molecular dynamics simulations. While the study does not investigate the use of an external electric field, it highlights the potential of IGO membranes for seawater desalination. Therefore, it is recommended to further investigate the use of electric fields in combination with IGO membranes to enhance their desalination performance.

Reduced graphene oxide membrane

Reduced graphene oxide (rGO) features a modified graphene structure characterized by a significant reduction in oxygen functional groups, particularly hydroxyl and epoxy groups[79,80]. These groups play a pivotal role in determining the material's chemical reactivity, surface properties, and electronic behavior[81,82]. The hydroxyl and epoxy groups in GOMs can significantly affect their water desalination performance[76,83]. The hydroxyl groups are hydrophilic and can form hydrogen bonds with water molecules, while the epoxy groups are hydrophobic and can repel water molecules. The presence of these oxygen-containing groups can affect the water permeation and salt rejection of GOMs. A relevant study was done by ref. 84 wherein the researchers studied hydroxyl/epoxy group's effects on water desalination through the spectacle of molecular simulations for lamellar GOMs. The study advocated the presence of hydroxy groups for water permeation through GOMs while concluding that water permeation is mitigated by the presence of epoxy groups. It was also found that salt rejection increases when epoxy groups are present.

To eliminate the oxygen-containing groups or alter the epoxy: hydroxyl ratio in GOMs, various methods have been proposed, including chemical reduction, thermal treatment, and functionalization with other molecules[79,82]. These methods can modify the surface chemistry and structure of GOMs, leading to improved water desalination performance.

However, it is important to note that these methods can also affect the mechanical and structural stability of GOMs, which can impact their long-term performance and durability. Overall, understanding the effect of hydroxyl/epoxy groups on water desalination through GOMs is crucial for designing and optimizing membrane materials for efficient water treatment applications. Further research is needed to explore new methods for modifying the surface chemistry and structure of GOMs to enhance their water desalination performance while maintaining their mechanical and structural stability[80,84].

A rise in temperature can facilitate the thermal deoxygenation of GO. However, this process uses a lot of energy, and the level of oxidation is challenging to regulate. With the addition of reducing agents such as metal hydrides ($NaBH_4$), hydrazine (N_2H_4), and hydro-iodic acid (HI), GO can undergo chemical reduction at low temperatures[85]. Targeting various oxygen functional groups help these agents to effectively manage the reduction reaction, and the water permeability could be maintained while creating angstrom-level channels that are appropriate for the separation at the ion level by utilizing the reduced functionalized GO[85]. The reducing agents might also shrink the as-fabricated GO membranes, resulting in lower nanochannel diameters and increased membrane hydrophobicity. Due to their reduced swelling, smaller nanochannels, and increased resilience in hostile chemical or aqueous environments, rGO membranes with lower oxygen functional groups can offer greater performances under explicit molecular sieving[86,87]. The intrinsic nanopores present on the rGO membrane as a consequence of reduction processes make them a suitable candidate for separation-related applications (size exclusion) as an ultrathin-film membrane[88]. Also, to obtain a high-performance rGO membrane, it is necessary to control the nanopores forming on the membrane surface while understanding the formation process behind them at an atomic level. The production of rGO/GO materials on a larger scale is desirable because they serve as a better alternative to pristine graphene. Their solution-based processing technology makes them easier. However, their ability to serve as an ultrathin membrane has been overlooked. The reduction process retains the defect on rGO while helping in getting rid of the oxygen-containing groups employing thermal, chemical, and electrochemical approaches[89,90]. To repair these defects and produce performance close to pristine graphene, many researchers have attempted to find an approach while following the report published by Zhou et al. on peeled-off graphene in 2002[91,92]. Zhang et al., in another study, recognized an rGO nanocomposite from a family of ultrafine metal oxide synthesized via heterogeneous nucleation and diffusion-controlled dye nanofiltration growth process. The functional groups on the GO surface, which contain oxygen, act as a heterogeneous nucleation site for producing high-density metal oxide nanoparticles of sub-3 nm size. These nanoparticles increase the lateral tortuous path, increase the vertical interlayer spacing (water permeability ~225 $L\ m^{-2}/h\ bar^{-1}$), enhance selectivity up to 98% (MB size exclusion separation), and help in forming a stable colloidal solution for membrane fabrication while inhibiting the wrinkles present on rGO nanosheets[93]. Huang et al.[94] also visualized GO defects and followed the steaming etching method to further increase the number of defects. This results in porous graphene having defects of different shapes and sizes despite the sp^3-carbon domains. These pores further enhance the mass transfer rate making porous graphene a suitable candidate for water desalination[95]. While concerning the commercial application of these materials, low-cost production at a large scale serves as the bottleneck. Thus, this mandates the economical synthesis methods for porous graphene to probe its physical and chemical properties[26]. A recent study by Zhou et al. demonstrated a porous graphene synthesis approach employing GO as a source for graphene being etched by polyoxometalates or oxometallates through a carbothermal reaction[64]. Various amounts of these polyoxometalates or oxometallates are employed for nitrogen doping porous graphene sheets for pore engineering[95]. These porous graphenes, as a result, would have improved mass transfer due to path shortening. Moreover, it is essential to discuss in detail the different process variables that one can think of tailoring while preparing these atomically thick membranes for separation-related applications. Thus, in the upcoming section, we have focused more on highlighting those variables that may act as a guiding beacon for the upcoming researchers in this field.

Effect of total oxygen concentration and functional groups on rGO nanopores

The production of rGO membranes under restricted conditions yields effective separation and high permeation flux compared to the recently available membranes. Kim et al. employed Hummer's method for producing a multilayer graphene oxide by epitaxially growing oxidized graphene films on the C-terminated surface of a SiC wafer[96]. This study helps to understand the stability of multilayered GO from a structural and chemical perspective. Under a relaxation time of 35 days, these multilayer GO exhibited a metastable behavior, underwent spontaneous reduction, and chemical modification was found to be under the control of diffusion processes. According to Density Functional Theory calculations, the driving force for these modifications was observed to be the H species present on the oxidized graphitic sheets. The leftover excess of H species is first captivated by the epoxide groups, followed by hydroxyl groups which lead to the release of water molecules. Also, the epoxide group's reduction is more favored due to the presence of C-H species than the hydroxyl groups. Furthermore, this study introduces a new understanding of a route to curb the GO properties, structure, and chemistry that is imperative for its large-scale industrial application[97]. In another study by Lin and Grossman a particular focus on controlling the rGO nanopores was emphasized, yielding a relationship between the defect size (nanopore size) and synthesis parameters, such as functional groups and oxygen concentration[88]. The parent GO material having high epoxy: hydroxyl ratio produced larger nanopores into the prepared rGO material produced via reduction. Figure 3 portrays how functional groups and total oxygen concentration affects rGO nanopores at constant reduction temperature. Although the extent of reduction is apparently compromised due to the strain produced via epoxy functional groups, the carbon removal percentage is elevated substantially[98].

Effect of temperature reduction of temperature is another imperative parameter that influences the formation of nanopores[99]. High temperature imparts high kinetic energy to the structures that elevate the probability of overcoming the reaction barrier to activated complex or by-product formation[88]. In a recent study by Zhao et al., excellent separation performance for water and NaCl was achieved through a thermally rGO membrane demonstrating Na^+ blocking ability 1529 times better than the parent GO membrane as shown in Fig. 3c. It is also expected to be better than the traditionally produced rGO membranes via NH_3 or HI reduction. On employing a draw solution of 3M sucrose, the thermally reduced GO 795 nm thick depicted an ultrahigh rejection of >99.56% for Na^+ and water flux of 0.42 $L\ m^{-2}\ h^{-1}$[100]. Another work by Lin et al. showed that by promoting the carbon removal in rGO material, high temperature causes high reduction while forming large nanopores[88]. Thus, the rGO produced from GO sheets having very low oxygen concentration tend to have smaller nanopores that don't allow water molecules to pass through them, while on the contrary, the passage of water at high oxygen concentration is only allowed when the reduction temperature, as well as when the epoxy to hydroxyl ratio, is on the higher side. Also, very high process temperature and functional group ratio as a synthesis condition produces large nanopores that allow both salt and water molecules to easily pass through, that is not a desired RO process. A better optimization of rGO membrane synthesis parameter would yield a better desalination performance. In order to have an oxygen concentration of 33% in GO sheets, it is desirable to have a smaller functional group ratio in addition to having a lower value of reduction temperature. Tailoring the nanopore formation on rGO sheets become an[13] important consideration here for designing membranes[88].

Thus, the synthesis parameters incorporating extensive epoxy: hydroxyl ratio and high reduction temperature result in undesirable large pore size and broad pore distribution. Accurate pore size control and fine-tuning of synthesis parameters are thus the two important pillars for rGO fabrication and serve as an open topic for research in future.

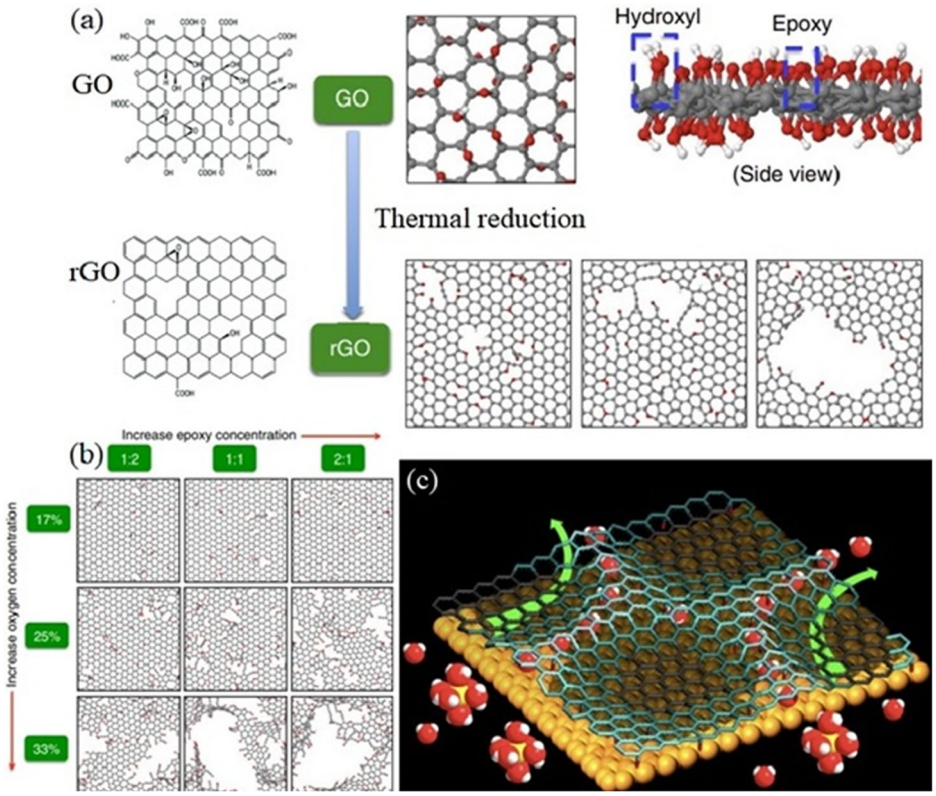

Fig. 3 | The figure depicts rGO formation from GO and effect of functional groups on rGO. **a** Schematic of the rGO formation[88] (**b**)Relationship between defect sizes and synthesis parameters[88]. This figure is from an open-access article distributed under the terms and conditions of the Creative Commons Attribution license. **c** Depiction of TrGO membrane's internal channels wherein water can penetrate and form a water channel. Reprinted under terms of the Creative Commons license from ref. 100. Copyright 2013 American Chemical Society. Description—visualizing the formation of rGO formation and TrGO structure.

Tuning the mechanical properties of GO membranes

Studying the structure of individual sheets and their interlayer interactions on the nanoscale is important as it impacts the colligative mechanical characteristics of such multilayer lamellar films[8]. Mao et al. found that by introducing in-plane porosity to a section of the sheets, it is possible to notice a drastic increment in the elastic moduli of GO films possessing multiple layers[101]. However, on the other hand, when Mao et al. conducted the same study for a single-layer GO sheet, it was found that the elastic modulus is dependent on porosity, and both these quantities are inversely related. When GO sheets possessing high porosity are assembled with pure sheets, much stiffer GO films are formed in such cases. It was concluded that due to the stacking of layers, the mechanical characteristics of perfectly un-etched GO sheets could not propagate and scale up to multilayered films from single-layered ones. Also, the porous GO sheets can be potentially efficient binders and promote packaging and interlayer interaction since they are considerably softer and more flexible, resulting in GO films with a higher modulus. Clean GO sheets are insufficient for packing requirements, which may appear counter-intuitive[49]. However, stacking properties of 2D sheets helps explain this as the sheets that constitute GO materials have extremely wide aspect ratios and can be easily folded and wrinkled when subjected to external stress[102]. As per the illustration in Fig. 4a, it can be understood that there will be an interference between the uneven topography and interlayer packing of adjacent sheets, owing to which the interlayer linkages will weaken, and ultimately, the load transfer will reduce[37]. However, if the sheets are free from wrinkles, it leads to the formation of multilayers tightly packed together, and thick slabs with high stiffness will be formed. These slabs apparently resist being packed together very tightly, and as seen in Fig. 4b, a desirable lamellar structure will form[13]. Therefore, it is doubtful that 2D sheets alone could produce lamellar films devoid of interlayer gaps. If the motive is to increase interlayer load transfer, employing porous GO sheets as the filler and binder offer more mechanical compliance. As the multiple GO sheets slide across each other and plastic deformation occurs in the film, the pure GO film's stiffness diminishes with increasing strain[8]. The addition of porous sheets may also strengthen the bonding between layers, increasing the film's resistance to tensile stress. On the other hand, when we have a 10 wt% mixed composite (5-h-etched GO sheets) film until the fracture point is reached, the film's stiffness stays consistent[99]. The separation performance of GOms is also somewhat influenced by the in-plane pore size and charge effect[95]. Also, some of the older studies on GOms prove that the molecular transport in stacked GO nanosheets takes place through the nanochannels between the GO nanosheets, and this can be seen in Fig. 4c. In the case of solutes with longer diameters (i.e., longer than the interlayer spacing), their passage through the GOm would not occur. The zero-separation bulk behavior, according to a simulation study using a double-layer GOM, occurred when the d-spacing continued to increase[50]. Also, only water vapor aligned in a monolayer GO can pass through a nanochannel made via vacuum filtration when they are dry (void spacing ~0.3 nm). In research by Joshi et al., such a GOm was submerged in an ionic solution, and it was discovered that owing to hydration, there was an increment in the GO spacing[5]. Joshi et al. also showed that all the species with a diameter greater than 0.9 nm were barred from entering the nanochannel (Fig. 4d)[50]. It was found that the LbL method, in contrast, is the best for adding an interlayer stabilizing force while layering. With changes in the number of LbL deposition cycles, controlling the GOms' thickness becomes easier. Theoretically, a sieving channel could be made from as few as two stacked GO layers. However, it is necessary to deposit additional GO layers to offset the adverse effects of uneven GO nanosheet deposition on the membrane's ability to sieve and eliminate other potential flaws. Synthesizing graphene membranes (monolayer) is challenging, however, following the LbL pathway to GOms' synthesis is a commercially affordable and scalable approach[50]. In another study by ref. 103, the surface structure of CS and CS/GO-1 membrane, as shown in Fig. 5, was investigated by XPS. It is well known that GO has a very high concentration of C-single bond, increasing carbon signal intensity. The C-NH-C bond quantity increased as a consequence of the reaction taking place between GO's epoxy group and CS's primary amino group. Additionally, due to the increased contribution of ammonium cation to N1s of CS/GO-1, it is evident that the ionization of the carboxyl group and protonation of the leading amino group happen at the same time, due to which there are strong electrostatic interactions. In

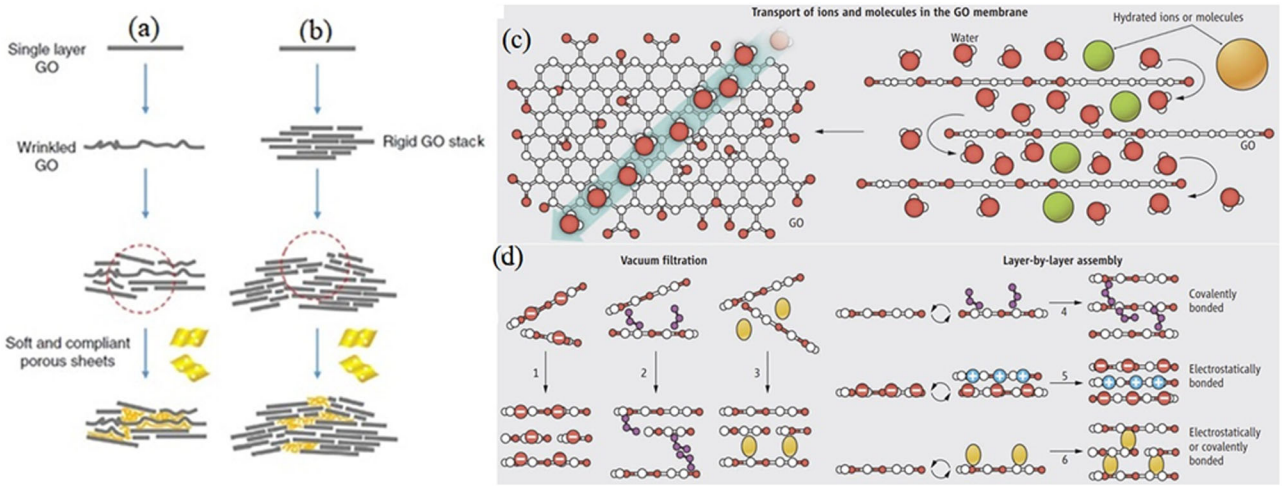

Fig. 4 | The illustration depicts the effect of stacking in GO sheets. a When being processed, it is considerably simpler to fold or make wrinkles on GO sheets. Due to this, the neighboring sheet's packing is disrupted, and (**b**) even though there is tight stacking in the sheets that are not wrinkled, the layers which are produced exhibit much less flexibility and more rigidity as they are attempting to prevent further conformal packing[166]. **c** This illustrates how the GO membrane is extremely fast at allowing water and small ions and molecules to pass through, but larger species are blocked[50]. **d** Techniques considered for manufacturing GO membranes; vacuum filtration to physically pack GO nanosheets; layer-by-layer assembly employing covalent bonds, electrostatic forces, or both to stabilize GO nanosheets[50]. This figure is from an open-access article distributed under the terms and conditions of the Creative Commons Attribution license. Description—studying the synthesis and structural manipulation of GO sheets.

Fig. 5a, C1s regions in the high-resolution spectra of CS are fitted with three components. The chitosan ring's carbon and N-C=O from acetylated moieties is both present in the peak at 287.9 eV. There are two peaks for N1 s (Fig. 4b), one of which is allocated to protonated amines (-NH^{3+})) at 401.2 eV and the other to C-single bond N and C=O-N bonds at 399.2 eV. In contrast, the carbon content of the CS/GO-1 MMM's single bond C, single bond N, and single bond O rose (Fig. 4c). Furthermore, the active charge -NH^{3+} contributes more to the N1 s of CS/GO-1 compared to that of CS in the N1 s spectrum (Fig. 4d) because GO has been added and is now exposed on the membrane surface, and thus the C1s between CS and CS/GO-1 differ[103].

Additionally, using small-flake graphene oxide (SFGO) membranes for nanofiltration offers several advantages, as highlighted in the research paper by ref. 104, wherein the focus was on developing SFGO membranes for Organic Solvent Nanofiltration (OSN) applications. In this, after engineering a less tortuous path for the transport of solvent molecules, the membrane was stabilized by intercalation with La^{3+}. The permeation of methanol was then tested for SFGO and Large-flake Graphene Oxide (LFGO) membranes, only to conclude that the permeation in SFGO was about three times as high as LFGO. Also, high selectivity for five different organic dyes was observed. The authors advocate the longevity of SFGO-La^{3+} membrane by subjecting it to realistic OSN conditions and concluded that the subjected membranes maintain their stability for more than 24 h. Among all the cations, La^{3+} cross-linked strongly to the membrane, given that it forms coordinate bonds with SFGO's oxygen-containing functional groups. A key takeaway of Nie et al.'s study is that in case of SFGO membranes, the solvent molecules travel through less tortuous paths, leading to faster transport, and for operations relevant to the purification of organic solvents, SFGO membranes are popular, given that they possess high permeability and selectivity for organic solvents[104].

Other than flake size modification and creating planar porosity within GO nanosheets, there are other methods to deal with the instability issue[86,105]: Physical confinement[18,106] and cross-linking by outside elements (such as organic and cationic compounds)[6,107] are two such methods. The GO membrane's durability in water can be potentially improved by reducing (partial) oxygen functional groups by strengthening pi-pi attraction and lowering electrostatic repulsion between the facing GO nanosheets[15]. Cross-linking or intercalating using nanomaterials (CNT)[105], organic molecules (polydopamine)[6], and cations (such as K^+ or La^{+3})[108] on the GO sheets produce interlocked nanosheets, unlike reduction that improves the interaction (cation-pi-pi interaction, complexation, etc.) while stabilizing the structure. Some examples of the recently used GO membranes for various separation-based applications have been discussed in Table 1.

GOm intercalation

The functionalized area of the GO membrane has pristine graphene channels between them that are responsible for permeating molecules and sieving properties; the interlayer d-spacing is the determining factor[37]. The interlayer d-spacing is a function of the surrounding humidity[5,32] and the GO laminates are typically swollen (d ~13.5 Å) when dispersed in water. Typically, 2–3 water molecules enter between individual GO sheets. A significant proportion of GO membranes (40–60%) do not have functionalization[109,110]. Again, several GO properties have been discussed to curb the separation efficiency, swelling effect, covalent crosslinking[13,111], partial reduction parameters[86] (hybrid rGO-titania membrane produced via ultraviolet reduction)[112], etc. Thus, intercalating GO sheets emerged as a new research idea where the contaminants are unintentionally introduced during GO processing and synthesis steps contributing towards membrane stability. Water transport could be easily modulated through these intercalants since they broaden the interlayer d-spacing by incorporating cationic porphyrin, soft polymers, polyelectrolyte brushes, etc.

Sometimes polymeric additives demonstrate limited water permeability enhancement mainly due to their random distribution and intrinsic elastoplastic behavior[113]. Also, the trade-off between selectivity and permeability instigates rejection deterioration[114]. Intercalant materials illustrating rigidity and high discursiveness property are benign for improving membrane permeability and tailoring the interlayer distance. However, an intercalation strategy producing the desired membrane is still a work in progress[115]. In a study by Wei et al., it was demonstrated that GO membranes reduce in thickness on applying water pressure the salt rejection improves due to steric effects[116]. The membranes reported NaCl rejection between 80–90% at 50 bar, which is higher than the previously reported research on GO membranes. Although, other investigators employed low NaCl concentration feed solution under a dead-end flow mode of operation[117]. The disadvantage of dead-end flow mode is that it builds up the concentration polarization layer at the membrane liquid interface. That is not the case with the crossflow mode of operation, thus amending the

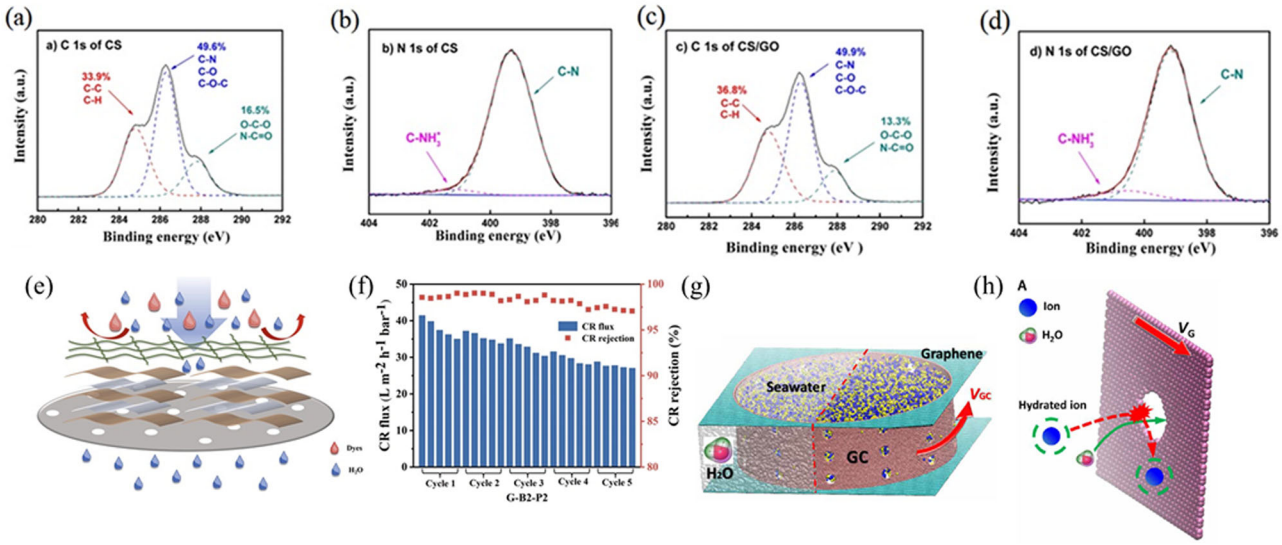

Fig. 5 | The figure depicts the characterization data of membranes along with rejection mechanism. The figure (**a**–**d**) illustrates XPS C1s and N1s spectra for two membranes, namely CS and CS/GO-1 membranes. Reprinted under terms of the Creative Commons license from ref. 103. Copyright 2018 Elsevier. **e** The figure depicts the mechanism through which the separation of a dye happens, and the membrane depicted here is named G-B2-P2. **f** The figure depicts the plot of CR flux and CR rejection versus the durability of the membrane Reprinted under terms of the Creative Commons license from ref. 118. Copyright 2023 Elsevier. **g** Schematic illustration of graphene sheets (blue) to contain the draw solution and a nanostructured spinning GC (red) (having 36 pores with 2 nm diameter). **h** Representation of the paths of a hydrated ion and a water molecule that has been penetrated and is used to describe how slip-induced selectivity works[134]. This figure is from an open-access article distributed under the terms and conditions of the Creative Commons Attribution license. Description—characterization and performance analysis of two membrane systems.

membrane desalination performance. Yu et al.[118] proposed an approach to intercalate hexagonal boron nitride (h-BN) nanosheets between GO laminates. The proposed approach also portrayed a method to carry out polyethyleneimine's (PEI) modification on the surface of the membrane. This was done to render immense levels of stability to novel GO membranes which are used for nanofiltration. For a range of dyes, the h-BN-GO nanocomposite membrane depicted highly efficient separations. Yu et al. also showed that at low pressure conditions, ~1 bar, the nanocomposite membrane had a higher permeability than the original membrane and the water flux (pure) of the original one was 722% lower than the nanocomposite membrane. It was also concluded that the dye's molecular weight and the dye's flux were related in an inverse proportion. In the case of the methylene blue (MB) dye, the one with the least molecular weight had the smallest magnitude of rejection, and the presence of molecular sieves in dye removal is attributed as the reason for this. In Fig. 5e, the membrane's mechanism for dye separation has been depicted. When membranes are used for commercial purposes, it is important that they possess great durability, otherwise the cost of operation would increase. So, Yu et al. conducted some cycling tests to evaluate if the proposed nanocomposite membrane can be used for longer times. As mentioned in Fig. 5f, the proposed membrane remained stable even after several cycles[118]. These (chemical) efforts may run across certain connected defects, notwithstanding significant progress. In addition to problems between GO nanosheets, vacuum-assembled GO membranes are susceptible to peeling off from the underlying substrate because of insufficient interfacial adhesion, which minimizes their strength and lifespan. In research by Morelos-Gomez et al., the reasons for GO membrane's stability in crossflow conditions were discovered[119]. Other research recently described a physical fixation technique that may stabilize GO membranes by applying a force that is opposed to the direction in which the GO nanosheets are inflating. It is still quite challenging to stabilize GO membranes. These and more novel and straightforward methods for improved stabilization are still needed. Vertically aligned GO has recently been used to produce high water penetration and strong salt rejection (>90%)[120]. However, its production is arduous to scale up at a cheap cost. Thus, a different technique, like spray coating, may build simple, scalable thin GO membranes.

Dye intercalants. Dissolved ions and molecules have the potential to reach the interlayer region and undergo significant adsorption as the GO structure swells[120]. Sorption of ions and molecules is a test method that may be used to confirm the GO interlayer distance in solutions[121]. The ability of ordinary dye molecules to enter the GO interlayer region is particularly intriguing to investigate. For instance, hydrated/solvated MB ions are bigger than permeation channels in various investigations, which prevents diffusion through the membrane[38,122]. These investigations did not take into consideration the strong sorption capacity of graphite oxides toward dyes. In a recent work by Nordenström et al., the sorption of MB by thin GO films was found to be greater (substantially) than the sorption of Crystal violet (CV) and Rose Bengal (RB)[123]. In Fig. 6a, it has been shown that the geometrical differences between planar MB and fundamentally non-flat CV and RB molecules cause this effect. The shapes of CV and RB, which are twisted and fundamentally not flat, hinder their intercalation. Owing to a collation of considerable interlayer distance expansion and sorption capacity, the intercalation of MB into the GO framework occurs. Therefore, it can be said that the molecules' hydration radius is not the primary factor influencing their ability to penetrate the GO interlayer region.

Intercalating-conjugated polycyclic cations provide several benefits. Their highly rigid 2D polycyclic backbone architectures, with a minimal thickness of less than 0.4 nm, provide enhanced control over the actual interlayer spacing of GO. Additionally, the distinctive microstructures produced by their stacking behavior impacts the rejection of solutes through vertical and lateral alterations. Even after being "flattened" by graphene complexation[115], other possible intercalants, like porphyrins[124], don't typically have a rigid two-dimensional backbone structure because of significant steric effects. Polycyclic compounds are widely available, and many of them, like TBO, are used in industry. However, in the case of porphyrins, there is a more significant capital cost associated with their synthesis and industrial usage. In the latest work, Wang et al. showed that conjugated polycyclic

Table 1 | A variety of graphene oxide/hybrid graphene oxide membranes for salt and dye rejection

Membrane category	Synthesis method	Mode of operation (operating pressure)	Rejection %	Dye/salt (charge)	Permeance (L m^{-2} h^{-1} bar^{-1})	Reference
rGO-TA	Pressure-driven filtration	home-made dead-end vacuum filtration device (1 bar)	~ 100 100 76 ± 5 81 ± 5	DW deionized water (N) RB rhodamine B (+) MLB methylene blue (+) EB Evans blue (−)	10,191 ± 30 2547 ± 20 2972 ± 20 2547 ± 20 1415 ± 20	[149]
rGO-TH	Pressure-driven filtration	home-made dead-end vacuum filtration device (1 bar)	~ 100 99 ± 1 71 ± 5 67 ± 5	DW deionized water (N) RB rhodamine B (+) MLB methylene blue (+) MB methyl blue (−) EB Evans blue (−)	10,720 ± 30 3612 ± 20 8526 ± 30 10,602 ± 30 10,520 ± 30	[149]
GO/TiO_2-PSS	Pressure-assisted filtration-deposition followed by dip coating	self-designed filtration device (2 bar)	93.2 93.9	$MgCl_2$ Na_2SO_4	51.2 56.8	[127]
ZIF-8@f-GOm	Vacuum filtration-ice templating	cross-flow nanofiltration system (1–7 bar)	100	MB (perfect)	49.8	[133]
CuTz-1/GO	Vacuum filtration	crossflow (4 bar)	98.2 94.9	DR MB	40.2	[150]
a-$BN_{2.0}$/GO	Pressure-assisted filtration	dead-end separation cell (20.68 bar)	99.98	MB	0.20	[151]
NH_2-Fe_3O_4/GO	Vacuum filtration	cross-flow circulation system (5 bar)	94 70 75 9.8 15 32	CRMB MO $MgCl_2$ NaCl Na_2SO_4	15.6	[152]
g-C_3N_4NT/rGO	Vacuum filtration	dead-end filtration (4.5 bar)	98.5	RhB	4.77	[153]
MoS_2/GO	Pressure-assisted filtration	amicon pressurized cell filtration (1 bar)	97.4 65.2 43.2	MB Na_2SO_4 NaCl	10.2	[154]
$OCNT_{s1}/GO_{10}$	Layer-by-layer self-assembly	cross flow system (1 bar)	99.3	MB	7.2	[155]
TiO_2/rGO/PES	Phase inversion	dead-end filtration (3 bar)	81 95	RB DY	9	[156]
STB_2@GO	Self-assembly	dead-end filtration (5 bar)	99.3 98.5	VB EB	9.14	[126]
CNTs/ GO	Vacuum filtration	dead-end filtration (3 bar)	27.5 44.4 - 46.2	Methyl orange Titan yellow Pure water Chlorazol black	61.2 57.6 66.5 58.2	[157]
SWCNT /GO	Vacuum filtration	vacuum filter apparatus (1 bar)	98.6 98.7 97.4	CBB BSA RB	720 ± 50 600 ± 30 710 ± 50	[158]
PDA Coated rGo membrane	Layer-by-layer self-assembly	forward osmosis (concentration gradient)	92	NaCl	36.6	[159]
GO/ DMAc/PVDF	Phase inversion	dead-end filtration (1 bar)	79	BSA	26.49	[160]

cations, TBO, are firmly attached to GO due to pi-pi and ionic attractions with the GO sheets. The authors mentioned that owing to these attractive forces, there might be a reduction in interlayer swelling. These attractions might also provide adjustable steric barriers in GO's interlayer galleries. Due to this, there might be shrinkage in the lateral spaces for hydrated ions, enhancing the route's tortuosity during molecular transport. (Fig. 6b) Monomeric binding modestly reduces interlayer gap for low and high TBO concentrations, but H-dimeric or higher order aggregate TBO binding significantly widens interlayer space. Therefore, the pi-intercalated GO-TBO membrane microstructures allow for the regulation of solute transport through changes in the interlayer gaps' lateral transport paths and their vertical interlayer spacing (as shown in Fig. 6 c and d). Consequently, dyes can aid in rejecting salt, and forthcoming scientists must explore various dye structures compatible with the membrane layers of GO[120].

Borates intercalation

Borates can covalently interact with the functional groups of GO, which contain oxygen, at different pH values. They are ecologically benign; thus, they have drawn much interest as an inorganic crosslinker. Currently, most investigations based on the crosslinking of borates with GO have been done to develop strong materials and high-barrier composite films, and it has rarely ever been used for water purification, though. Han et al. employed a novel assessment technique to show that borate and GO have a potent cross-linking connection[125]. Furthermore, it was shown that organic cross-linking did not improve the antioxidant activity of the GO membrane when borate cross-linking was used. In prior research, LbL-laminated GOms possessing good mechanical characteristics were created using borate ions[126]. Upon the crosslinking of GO with borate in a solution, a greater degree of intercalation may be attained. Hence, prior to preparing the membrane, it would be advisable to synthesize the intercalated nanocomposites in a solution. Additionally, no research has been done to study borate's utility in modifying the chemical characteristics of the membrane surface and d-spacing[126]. In research by Yan et al., GO nanosheets were intercalated with sodium tetraborate pentahydrate (STB) to create a nanocomposite (STB@GO). The findings indicate that when STB concentration grew (from 0 gram per liter to 1.6 gram per liter), the membranes' hydrophilicity and

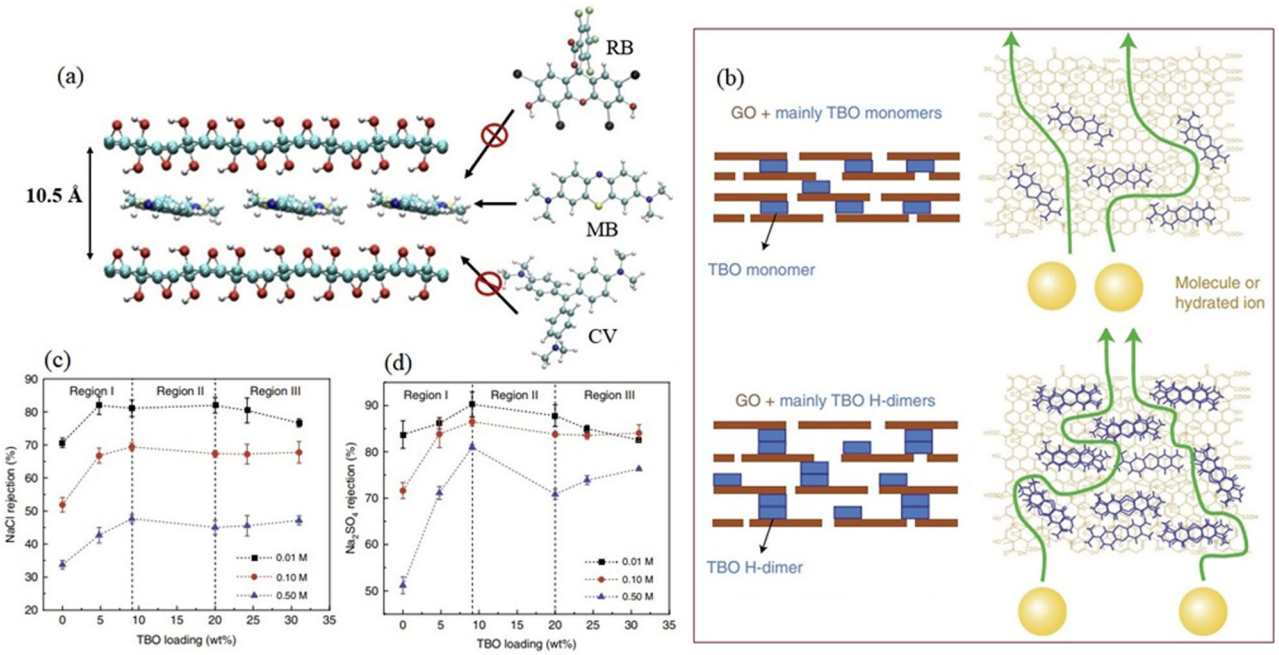

Fig. 6 | The figure shows the effect of intercalation in membranes. a Illustration of the GO structure with methylene blue intercalated in between the GO layers[123] This figure is from an open-access article distributed under the terms and conditions of the Creative Commons Attribution license. **b** Monomeric and stacked (H-dimeric) TBO aggregate, resulting in a significant increase in the interlayer d-spacing[120]. **c**, **d** The GO-TBO membrane salt (NaCl and Na2SO4) rejection has been plotted against TBO content for different feed concentrations Reprinted under terms of the Creative Commons license from ref. 120. Description—effect of intercalating molecules on the structure and rejection performance of GO membranes.

negative potential also increased. Nevertheless, the d-spacing demonstrated an initial rise to 1.347 nanometers and a subsequent drop to 0.904 nanometers. This demonstrated that adjusting the STB concentration might vary the membrane's chemical characteristics and d-spacing at the surface. The maximum flux was seen in the STB2@GO membrane with the largest d-spacing, showing that d-spacing had the most significant impact on the STB@GO membranes' ability to reject flux compared to the GO membrane[126].

Surface-charged graphene oxide membrane

Given the higher interaction energy barrier for GOms, the highly charged surfaces repel the co-ions showing high valency while simultaneously preventing the penetration of counter-ions possessing a lower valency. The purposefully controlled surface-charged GO membranes exhibit a notable improvement in ion rejection, with water permeance which inherent such high water permeance values that the performance threshold of cutting-edge nanofiltration membranes is surpassed. The domains of water transport, biomimetic ion channels and biosensors, ion batteries, and energy conversions can all benefit from this simple and scalable surface charge management method[127].

In the work presented by Zhang et al., a method to achieve controlled ionic transport has been proposed using GOms. Also, in this work, the process has been designed so that the transport takes place without obstructing water filtration. Tunable charges associated with the pre-stacked GO laminate's surface exhibited a strongly repellant electrostatic force against the counter-ions possessing a single charge while suppressing mild electrostatic attraction toward doubly charged co-ions. Water may still pass freely through the membrane while preventing the transport of ions from typical AB^{2-} or A_2B^{-} type salts as shown in Fig. 7a. This prevention takes place by adjusting the interactions of charges between the surface of the membrane and water ions, as can be seen in Fig. 7b,c. The GO-PDDA membrane that had the highest positive charge possesses a surface charge density of $+1.8\ mC\ m^{-2}$ [128], while it was $2.32\ mC\ m^{-2}$ for the GO-PSS membrane possessing the most significant negative charge (Fig. 7c). Zhang et al., as well as Werber et al., increased the water permeance by almost four times by intercalating NPs into the GO laminates, which are charged on their surfaces, and this was done based on the salt's exclusion capacity[129,130]. This encouraging finding implies that the surface-charge management strategy could potentially enhance water transport by adequately tuning the GO nanochannels.

Nanomaterial-based GOms

Nanocrystals are intended to be added to the edges of GO nanosheets for two reasons. Firstly, it is done so that the enlarged laminate structure's mechanical strength can be enhanced, and the problems associated with instability can be mitigated. Secondly, nanocrystals are added so that the defects in the frameworks can be filled and the undesirable solute's permeation can be blocked while not obstructing the permeation of water. MD simulations show NTs have the most significant promise for RO desalination[12].

Recently, filtration-produced GO membranes showed NaCl rejection of around 60 percent 165, and adding cylindrical nanoparticles can boost the water permeate flow of membranes on GO[12,56]. When GO and carbon nanotubes were combined, the membranes could endure shear flow while in use. Unfortunately, the manufactured CNT-based membranes (having diameters in the range of 1.6–7 nm) cannot repudiate the sub-2 nm particles, implying that they are not yet appropriate for seawater desalination at this time except in uniform single-walled form. Another nanocrystal chosen to accomplish these aims is ZIF-8 because of its capacity to form in situ crystals under favorable circumstances, its low frictional barrier to water transport, and its water-solute solid selectivity[119].

Membranes made of different nanomaterials have also been created. For example, completely hydrated MoS_2 membranes with 0.9 nm of free space display high water permeability of up to $6\ L\ cm^{-2}\ day^{-1}\ MPa^{-1}$, and about a 90% ionic rejection[131]. To achieve a permeability of $2.4\ L\ cm^{-2}\ day^{-1}\ MPa^{-1}$ with 86% salt rejection, Yang et al. recently created a graphene-nano mesh per CNT-hybrid membrane, and the pore size was about 0.63 nm[28]. Nano-porous graphene membranes possessing a charged monolayer whose pore diameter is 1.44 nm have salt rejection effectiveness between 93% and 100%, while the necessary pressure drop is significantly decreased[132].

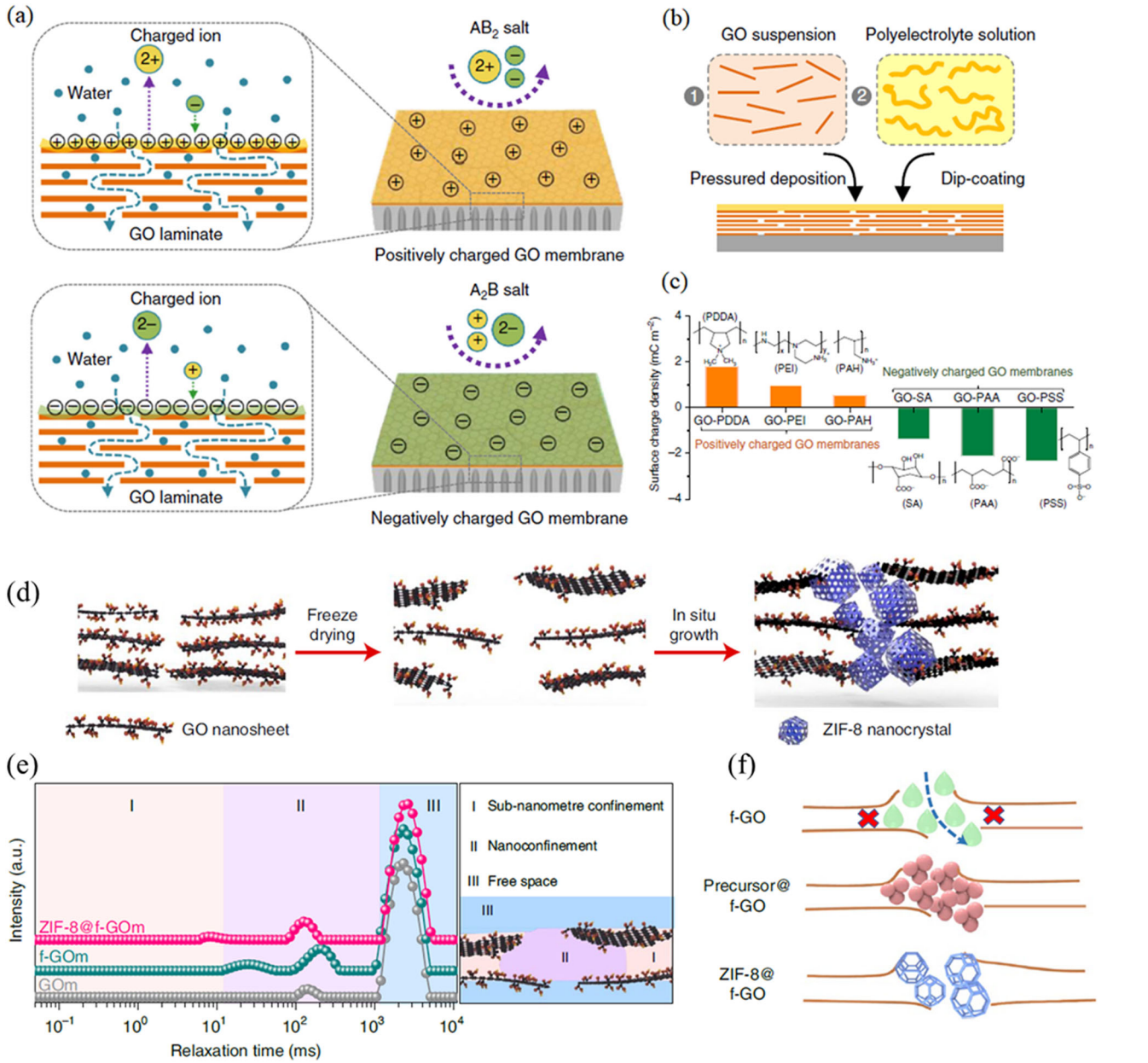

Fig. 7 | Effect of surface charge and nanocatalysts on GO membranes. a The figure depicts the process of engineering the surface of GOms to attain controllable ionic transport through the polyelectrolytic coating of the GO laminate's surface. **b** The figure depicts a method to fabricate surface-charged GOms. **c** The figure shows the surface-charged GOms' surface charge densities, which are based on calculations done using the Gouy–Chapman theory[127]. This figure is from an open-access article distributed under the terms and conditions of the Creative Commons Attribution license. **d** Freeze drying of GO framework while growing ZIF-8 nanocrystals that act as mechanical support within the microporous defect. **e** GOm and f-GOm 1 H time-domain NMR spectra with MeOH being a probe molecule. **f** Illustration of Zhang et al.'s method to place ZIF-8 nanoparticles precisely at the GO nanochannel edges[133]. This figure is from an open-access article distributed under the terms and conditions of the Creative Commons Attribution license. Description—controlling ion transport and enhancing mechanical support in GO membranes.

A zeolitic imidazolate framework-8 (ZIF-8)-nanocrystal-hybridized GOm was found to be very stable and ultra-permeable by Zhang et al., as seen in Fig. 7d. ZIF-8 was first in situ crystallized at the nanosheet edges. The wetted GO framework was freeze-dried using the ice-templating (IT) process, which led to the formation of an f-GOm, which has increased interlayer spacings for decreased mass transport resistance to water. But using methanol (MeOH)/NH_3H_2O to adjust the balance between crystal nucleation and growth allowed for fine control of ZIF-8 growth. All GO-based membranes have a large population in the time domain of 103–104 ms in their transverse relaxation times (Fig. 7e), which is a sign that the membrane is surrounded by free MeOH molecules (free space). Further evidence that MeOH molecules cannot pass through the laminated GO nanosheets is provided by the fact that there is an absence of signal from the sub-nanometer confinement zone. ZIF-8 development is limited to the flaws in the porous f-GOm (Fig. 7f). The interlayer spacings are widened by selectively developing ZIF-8 in the microporous flaws, which also gives the laminate framework mechanical integrity. This results in a stable microstructure with a water permeability of 60 L/m^2/hour/bar (30 times greater than GOm) for 180 h. Additionally, ZIF-8 growth improved microporous flaws, which boosted the methyl blue molecules' perm selectivity by a factor of six[133]. In the work by Zhang et al., a unique desalination process demonstrated temporal selectivity by employing slip-induced separation. This is done to overcome the trade-off between permeability and selectivity. With enormous holes that are 2–5 times bigger than the hydrated sodium

ions' diameter, rotating porous monolayer graphene cylinders (GC) are used to desalinate water (Fig. 5g).

The salt repudiation is greatly improved at the water-GC contact by the boundary slip. Under pressure created by the centrifuge, the huge nanopores produce an ultrahigh water flux. As a result, the trade-off between permeability and selectivity is eliminated by this unique slip-induced separation, which also overcomes the traditional pore size restriction. The rotating porous graphene demonstrates a 98.5% salt rejection and a water flow rate of over 3000 L cm^{-2} day^{-1}. A water molecule may be shown graphically passing through the pore while a hydrated ion bounces off the pore's edge in Fig. 5h. The resulting distribution (radial) of concentration and density for water molecules and ions also shows no concentration polarization. The water permeability in this study surpassed that of the GCNT hybrid membrane by nearly threefold, maintaining a salt rejection of 86%[134].

This achievement finds resonance in the research by ref. 77, where GO/HKUST-1 MOF membranes were explored for seawater desalination using pervaporation. The simulations indicated substantial water flux with HKUST-1 featuring single and double layers of GO. This suggests that MOFs could potentially be used to create GO composite membranes for desalination. However, further research is needed to explore this possibility. Another study by Zhang et al. investigated the use of graphene oxide-reduced graphene oxide-titanium dioxide (Geo-rGO-TiO_2) nanocomposites for seawater desalination via pervaporation. The study found that the Geo-rGO-TiO_2 nanocomposite membranes had high water flux and salt rejection, making them a promising candidate for seawater desalination. Overall, MOFs and graphene-based composites show potential for use in desalination membranes, but more research is needed to fully explore their capabilities. Yang et al., in one of their works, introduced a graphene nanomesh possessing a singular layer that is sustained by a matrix of single-walled carbon nanotubes. As shown in Fig. 8a–f, the mechanically robust, linked SWNT webs[135] function as a microscopic scaffolding to hold the supported graphene nano-mesh and exhibit a strong p–p interaction with the supported graphene nanomesh. This structure may be considered Voronoi cells[14,136] of a Voronoi diagram (Fig. 8b. According to Fig. 8d, the GNM/SWNT membrane demonstrated that the salt rejection is strong and lies between 85.2 and 93.4%. Also, the selectivity was in the following order: Na_2SO_4 > $MgCl_2$ > NaCl > KCl. These investigations imply that the GNM/SWNT membrane's ability to reject salt results from sub-nanometer-sized holes that enable efficient segregation through the size exclusion effect. In this study, the GNM/SWNT membrane's salt rejection (>86% NaCl) was found to be much greater than most GOms (19–42%)[15,137]. When commercial NF membranes are compared with commercial RO membranes, the salt rejection by the latter is significantly higher[138]. Thus, the conditions for the growth of graphene and the process of creating pores might be optimized to reduce cracks and flaws and increase the distribution of pore size, which would further enhance the salt rejection efficiency of the GNM/SWNT membranes. The hybrid membranes address the crucial trade-off between the permeation of water and the rejection of solute in the case of traditional desalination membranes. Their notable attributes, including high water permeance, impressive size selectivity, and exceptional antifouling properties, render them particularly appealing for efficient and energy-effective water treatment[131].

Another avenue to bolster solute rejection involves an alternative membrane design: the incorporation of one-dimensional (1D) multi-walled carbon nanotubes (MWCNTs) within 2D graphene oxide (GO) nanochannels[75,139]. This design creates membranes with hyperlooping pathways, allowing for efficient filtration and separation processes. By merging MWCNTs with GO nanochannels, a synergistic enhancement arises, encompassing high permeability, selectivity, and mechanical stability.

This concept is notably examined in the study by ref. 137, which delves into the utilization of hyperlooping carbon nanotube-graphene oxide nano architectonics as membranes designed for ultrafast OSN. The study demonstrates the superior performance of these membranes in terms of high flux and excellent separation efficiency. Additionally, other studies have investigated the incorporation of carbon nanotubes (CNTs) in membrane technology for various applications, including water purification, desalination, and gas separation[84,137,140]. CNTs offer unique properties such as anti-biofouling, salt rejection capability, exceptional electrical conductivity, and mechanical strength, making them promising materials for membrane design. Overall, the use of carbon nanotubes, graphene oxide, and their combinations in membrane architectures shows great potential for improving solute rejection and enhancing membrane performance in

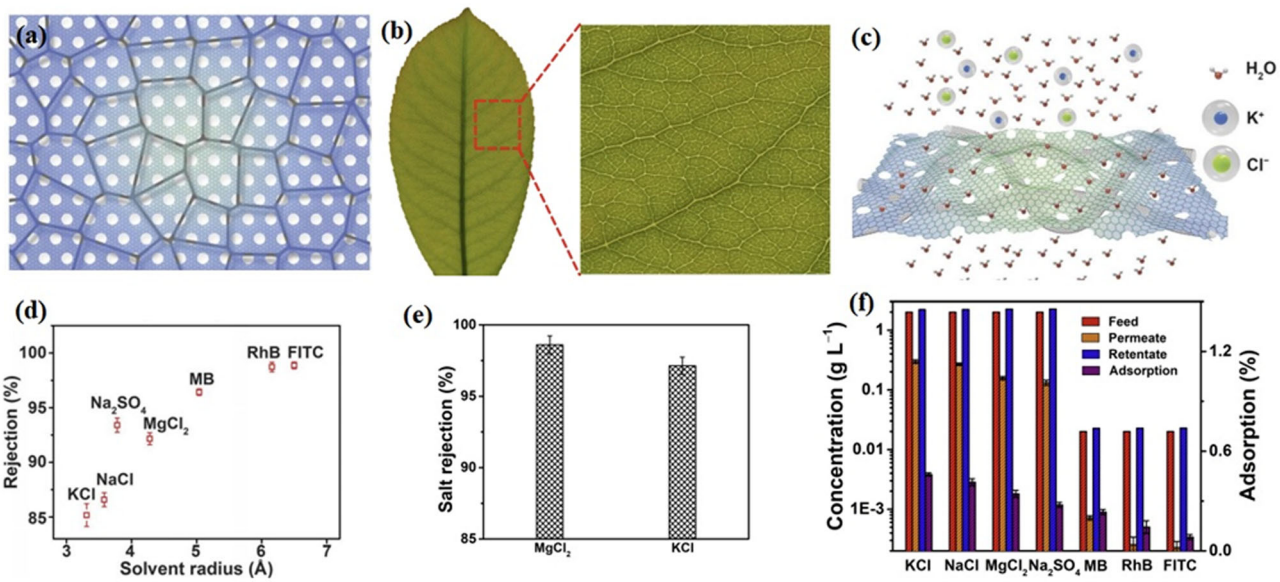

Fig. 8 | The figure depicts hybrid membranes and their rejection capabilities. a A structural model of the single-layer GNM/SWNT hybrid membrane supported by SWNT networks. **b** A photograph of a leaf fragment with the vein-mesophyll structure. **c** The GNM/SWNT hybrid membrane's structural model for size exclusion nanofiltration. **d** Rejection of KCl, NaCl, Na_2SO_4, $MgCl_2$, MB, RhB, and FITC by the GNM/SWNT membrane. **e** $MgCl_2$ and KCl rejection by salt. **f** Examining the GNM/SWNT membrane's capacity to adsorb salt and dye molecules during filtering experiments[131]. This figure is from an open-access article distributed under the terms and conditions of the Creative Commons Attribution license. Description—structural models and performance evaluation of GNM/SWNT hybrid membrane for size exclusion nanofiltration.

Table 2 | Comparison of high-water stability GOms membranes

Membrane category	Synthesis method	Rejection %	Dye/salt (charge)	Permeance (L/m².hr.bar)	Remarks	Reference
MCE/c-GO-PVA	Pressure assisted filtration	99.99	10 wt.% NaCl	98	High stability and resistance sonication destruction	[161]
α-Al_2O_3/PDA/GO	Vacuum-assisted filtration	99.7	3.5 wt.% NaCl	48.4	High stability upto 336 h	[162]
PTFE/GO-PVDF	Casting	99.9	3500–34,000 ppm NaCl	97	High stability under more salt concentration with 90 days run.	[163]
GO	Cross-linkage	99 ± 1 98 ± 1 98 ± 2 99 ± 1	RB MLB MB EB	21 ± 3 25 ± 3 14 ± 3 12 ± 3	Highly stable	[164]
(PDA@PEI/GO/PDA)/PES	Dip coating	9482	DY86	59.58	Highly stable	[165]

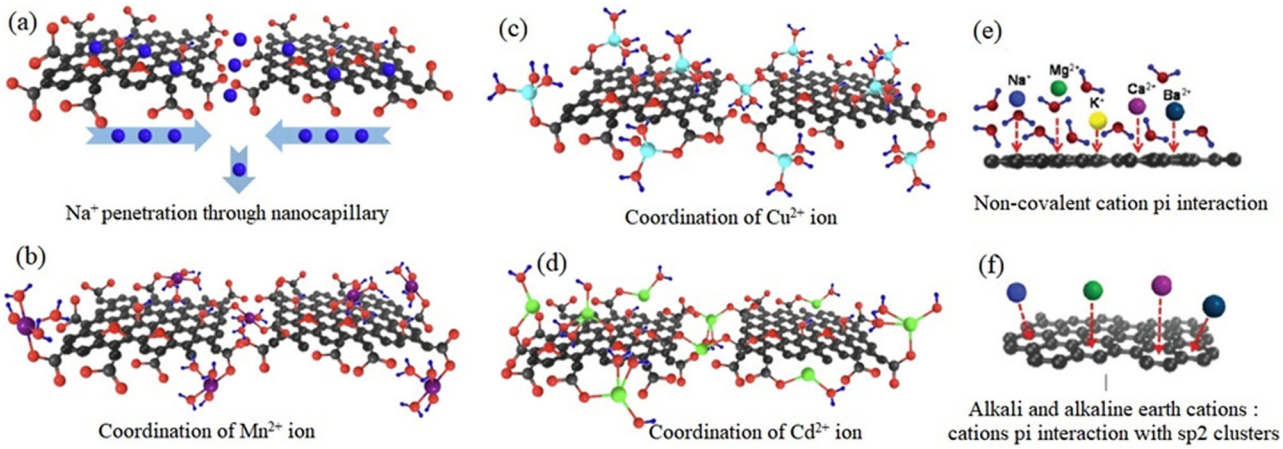

Fig. 9 | The figure explains the interactions of ions with the membranes. **a**–**d** Coordination of different ions (**a**) Na^+ and (**b**) Cu^{2+}. **e**, **f** Alkali and alkaline earth cation-p interactions with GO sheets Reprinted under terms of the Creative Commons license from ref. 142. Description—coordination of Ions with GO Sheets: insights into cation-P interactions.

various filtration and separation processes. Further research and development in this area can lead to the design of more efficient and advanced membranes for various applications, while also addressing the challenge of achieving precise and consistent creation of defect-free sub-nanometer pores with a radius below 0.45 nm and maintaining controlled interlayer distances at the same scale. The performance demonstrated by the innovative GO membranes up to now represents a compromise between permeability and selectivity, similar to conventional membrane systems. Methods such as vacuum filtration, drop-casting, and dip coating on a small scale provide a straightforward route for delving into the chemistry and transport mechanisms of Graphene Oxide (GO) membranes. Meanwhile, spin coating and pressure-assisted assembly achieve a high degree of organization among the GO sheets. On the other hand, when dealing with larger scales, approaches like slot-die and bar coating offer distinct advantages by orienting the flakes through the application of shear force on planar surfaces. In contrast, spray coating is better suited for non-uniform substrates. Moreover, the performance of GO membranes undergoes alterations under different environmental conditions. To offer a comprehensive perspective on this matter, an illustrative Table 2 has been provided, encompassing pertinent information regarding the behavior of GO membranes, while emphasizing their stability.

Challenges and perspective

As mentioned in the above sections, membranes must fulfill specific criteria to be used on the commercial or laboratory scale. Among several popular membranes, GOms gained popularity since they offer very high values of molecular separation and ion selectivity[141]. Nevertheless, in addition to the physical electrostatic impact, chemical processes also play a role in the interaction between GO and ions. Since the functional groups consisting of oxygen are capable to form a cluster, this leads to the formation of tiny sp^2 areas, and they become isolated inside the sp^3 matrix. On the sp^3 matrix, the existence of strong coordination between transition metal ions and the oxygen-containing functional groups is made possible by the presence of d-electrons (Fig. 9a–d). Nevertheless, when interacting with sp^2 clusters, cation-p interactions are preferred by alkali cations and alkaline earth cations that lack d-electrons (Fig. 9e, f)[142]. As a result, the following consequences of desalination by GOm have indeed been addressed:

(a) Wall surface effect: When there is a decrement in the channel and pore sizes, it converts into a free space where the fluid transports through the membrane. Wall surface effect partly governs the selectivity and permeability of a membrane. To enhance selectivity, it can induce preferential adsorption of certain molecules on the membrane surface. On the other hand, having a stronger wall surface effect will catalyze the diffusion of molecules, which leads to an increment in the membrane's permeability.

(b) Screening effect: There is the presence of an electrostatic interaction between the GOms, which happens because the functional group containing oxygen on the negatively charged GO sheet's surface gets protonated. These electrostatic forces are caused because of the screening effect brought on by the addition of extra ions. Increased electrostatic repulsion forces are due to an increase in surface charge, while a rise in ionic concentration causes an increase in the screening

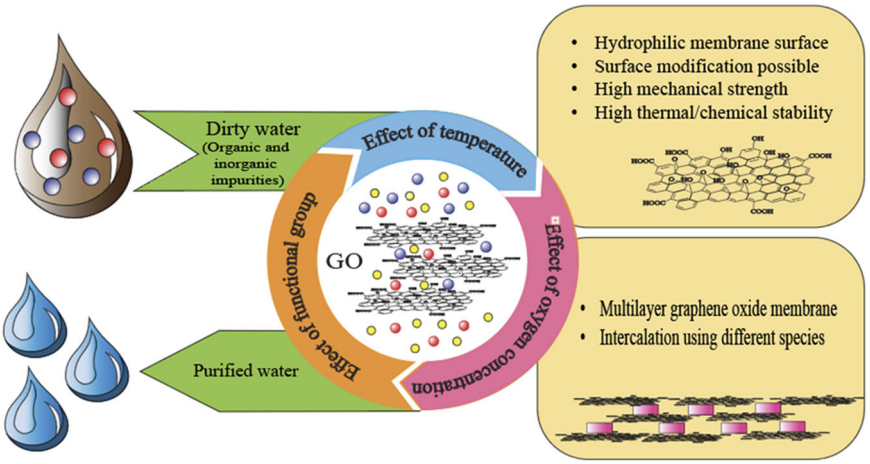

Fig. 10 | Factors influencing the performance of GO membrane in water purification. Description —lifecycle of polluted to clean water and the factors affecting this transition.

effect. From this angle, it is evident that GOms' lamellar structure and ion transport are influenced by the surface charges of GO sheets and the ionic content of dissolved salts. For GOms, in fact, other membranes too, there will be an improvement in selectivity due to a strong screening effect, and this will aid the process of selective separation of solutes. Supplementarily, a stronger screening effect will ensure the blocking of unwanted materials that might potentially damage the efficacy and longevity of the membrane through fouling.

(c) pH effect: The change in pH in the GO sheets and studying this change is typically helpful in assessing how surface charges have changed. In reality, when the pH of the solution rises, the carboxyl and hydroxyl groups deprotonate more readily, increasing the GO surface's negative charge. Consequently, it is beneficial to have the presence of an electrostatic interaction between metal ions and the GO surface.

(d) Horizontal defects: Assembled layer by layer, GO membranes may be impacted by horizontal defects. One of the GO's outstanding problems is the interlayer spacing, which can reduce selectivity if it is too broad or increase permeability if it is too small[143]. In the context of horizontal defects in GOms, selectivity, and permeability refer to the ability of the membrane to selectively allow certain substances to pass through while blocking others. Specifically, selectivity refers to the ability of the membrane to distinguish between different types of molecules or ions, while permeability refers to the rate at which a particular substance can pass through the membrane[4]. For example, a study on GOms found that they displayed intrinsic high water/ion selectivity, meaning that they were able to selectively allow water and certain ions to pass through while blocking others[4]. Another study on layered frameworks found that water permeability decreased significantly due to the tortuosity of the framework defects, which made it difficult for water to pass through[2]. Overall, the selectivity and permeability of GOms and other layered frameworks are important factors to consider when developing membrane-based separation technology, as membranes with superior selectivity and permeability are essential for efficient separation processes[3].

The acceptable interlayer spacing range that will not severely reduce sensitivity or permeability in GOms can vary depending on the specific application and the properties of the membrane. However, some studies suggest that the interlayer spacing of GOms should be precisely controlled within a certain range to achieve optimal performance. For example, a study suggests that the interlayer spacing of GO membranes should be confined between 11.4 and 13.4 Å to study the adsorption of ions with a diameter between 8 and 10 Å. Another study suggests that the interlayer spacing of GO membranes should fall into the range of 0.6–1.0 nm to achieve optimal water permeation.

Due to the impacts above, the water desalination sector has stringent requirements, making it more difficult for GO to be used as a membrane material. Despite these constraints and difficulties, GO presents a possible generation of separation membranes for accurate ionic sieving and super-high water flow. Due to the smaller size of the hydrated functional groups, rGO has also garnered much interest in reducing the interlayer gap. Nevertheless, it has been established that the laminates' significant graphitization and the structural damage not seen during reduction are to blame for the high impermeability. Additionally, intercalating small-sized ions to connect the stacked GO sheets holds significant potential for overcoming the hydration force and producing narrower nanochannels[144].

As a result, there is still a difficulty with water stability in exclusively GO or rGO membranes, with some potential answers, nevertheless. Efficient water desalination using GO membranes is challenging using the pressure filtering technique, according to a claim that sub-nanometer-sized channels are necessary for the GO membrane structure. Therefore, it is essential to properly design the pore channels in GO membranes because it will lead to the prevention of the movement of ions that are smaller in size. To fine-tune the membrane, more research is required (Fig. 10). To produce sub-nanometer channels inside membranes based on graphene, precise control of the pore size or inter-layer spacing must be made. Highly interlocked stacking, molecule intercalation, reduction treatment, etc. may be helpful to achieve this. Furthermore, it is anticipated that adjusting the flow direction and distance across the GO laminates or composites will improve the efficacy of the membrane separation. Addressing the challenges associated with graphene-based membranes for separation, including the stability of laminar membranes in crossflow scenarios and the establishment of reliable modules for ultra-thin few-layered membranes, is essential[3].

One of the key concerns in membrane separations is membrane fouling, and this problem is not central to graphene-based membranes. In fouling, unwanted materials accumulate on the membrane's surface and pores. This diminishes efficiency, longevity, and permeability while energy consumption increases[145,146]. There are many ways that have been discussed in the literature to catalyze the antifouling of membrane or prevent the fouling in the first place. These approaches include fabricating the membrane by blending multiple polymeric materials possessing distinct hydrophilicity[147], adding nanoparticles or other materials into the membrane matrix, coating the membrane with hydrophilic or zwitterionic materials, employing nanosheets with photocatalytic properties, etc. Further research and development efforts are necessary to improve the antifouling properties of GOms and enhance the efficiency and sustainability of membrane-based technologies.

Another concern that lingers around graphene-based membranes, which, of course, includes GO membranes, is their scalability. In 2013, Lockheed Martin claimed to have developed a graphene-based membrane capable of desalinating water "at a fraction of the cost of industry-standard RO systems".The potential commercial membrane was named perforene, wherein the active layer's thickness is at the atomic level. The study claims perforene to tolerate transmembrane pressures of hundreds of PSI, in addition to being extremely flexible and capable of tolerating high curvature

radii[148]. Even though perforene is deemed industrially affordable by Lockheed Martin, its claims met several criticisms[148]. Arguments related to defects and the inability to control them during industrial-scale production of large single-layered graphene-based sheets have also been made. It is challenging to manufacture nanocomposite membranes commercially while maintaining the minimum Quality Control requirements. Even if significant capital is invested and highly permeable graphene-based membranes are used, the permeability will keep increasing with time, leading to a decrease in separation efficiency. This would significantly minimize the efficacy of the plant. Another factor that would undoubtedly delay the transition of graphene-based membranes (including GO membranes) from the laboratory to the market is that most water treatment plants have been designed for membranes exhibiting lower permeability. Thus, newer plants would have to be constructed for highly permeable membranes. Not only would this add a significant capital burden on the plant, but it would also require a long time before we would commercially use graphene-based membranes. Compared to RO membranes used for desalination, graphene-based membranes can achieve 100% salt rejection at a permeability value of better than 10^{-9} m Pa^{-1} s^{-1}. While the ability of GO membranes has been scientifically proven, for it to replace RO membranes, there are many factors wherein there is good scope for improvement. Several articles in the literature have argued the benefits of commercially employing membranes with higher permeability, however at the same time, it is also necessary to mention that a highly permeable membrane leads to 10–20% improvement in energy demand in nanofiltration. Regarding the economics of nanofiltration, there is a decrement of less than 10% in the operational cost and thus, it might be beneficial to focus on other cost-cutting avenues if highly permeable membranes, such as GO membranes, are to be used commercially[2]. In summary, Graphene-based membranes are well-suited for creating nanofiltration (NF) membranes with ion-selective sieving capabilities, as many physical and chemical processes come into play during ion transport through specific membranes. However, the membranes' rejection performance is compromised as they tend to swell in aqueous environments. Therefore, this paper aims to illustrate all methods through which a graphene oxide membrane can be modified to obtain the necessary separation efficiency. We delve extensively into the impact of temperature, functional groups, and overall oxygen concentration on GOms. Additionally, several methods for adjusting the mechanical characteristics of GO have been described, considering the preparation techniques and membrane operating conditions. For single-layer porous graphene, multiple charged chemical functional groups have been added to the nanopore, which may effectively impede ion transport. The confluence of elements that leads to superior ionic selectivity necessitates careful planning when developing these separation-based membranes. Additionally, ion transport via graphene nanopores is better understood when considering the importance of the nanopore size and the effects of dehydration. On the contrary, several variables and their complex interactions impact ion transport through GO membranes. Ultimately, reviewing the role of nanomaterials in constructing multifunctional composite graphene membranes. These composite membranes exhibit enhanced mechanical strength and water permeability, holding significant potential for applications in the water treatment industry. Nevertheless, greater focus should be paid to studies into fabrication, related transport mechanisms, and the use of multifunctional composite membranes. Understanding constrained mass transport inside composite membranes is also crucial for modifying membrane separation performance, even though the transport behavior is complicated due to several effects operating in concert.

Data availability

All the data associated with this article will be made available via email through the corresponding author.

Received: 15 March 2023; Accepted: 11 March 2024;
Published online: 27 March 2024

References

1. Elimelech, M. & Phillip, W. A. The future of seawater desalination: energy, technology, and the environment. *Science* **333**, 712–717 (2011).
2. Boretti, A. et al. Outlook for graphene-based desalination membranes. *npj Clean Water* **1**, 1–11 (2018).
3. Liu, G., Jin, W. & Xu, N. Graphene-based membranes. *Chem. Soc. Rev.* **44**, 5016–5030 (2015).
4. Perreault, F., De Faria, A. F., Nejati, S. & Elimelech, M. Antimicrobial properties of graphene oxide nanosheets: why size matters. *ACS Nano* **9**, 7226–7236 (2015).
5. Joshi, R. K. et al. Precise and ultrafast molecular sieving through graphene oxide membranes. *Science* **343**, 752–754 (2014).
6. Guo, J. et al. Unravelling intercalation-regulated nanoconfinement for durably ultrafast sieving graphene oxide membranes. *J. Memb. Sci.* **619**, 118791 (2021).
7. Zhang, Y. et al. Ice-confined synthesis of highly ionized 3D-quasilayered polyamide nanofiltration membranes. *Science* **382**, 202–206 (2023).
8. Dikin, D. A. et al. Preparation and characterization of graphene oxide paper. *Nature* **448**, 457–460 (2007).
9. Chen, C. et al. Self-assembled free-standing graphite oxide membrane. *Adv. Mater.* **21**, 3007–3011 (2009).
10. Huang, L. et al. Reduced graphene oxide membranes for ultrafast organic solvent nanofiltration. *Adv. Mater.* **28**, 8669–8674 (2016).
11. Qiu, L. et al. Controllable corrugation of chemically converted graphene sheets in water and potential application for nanofiltration. *Chem. Commun.* **47**, 5810–5812 (2011).
12. Huang, H. et al. Ultrafast viscous water flow through nanostrand-channelled graphene oxide membranes. *Nat. Commun.* **4**, 1–9 (2013).
13. Hu, M. & Mi, B. Enabling graphene oxide nanosheets as water separation membranes. *Environ. Sci. Technol.* **47**, 3715–3723 (2013).
14. Akbari, A. et al. Large-area graphene-based nanofiltration membranes by shear alignment of discotic nematic liquid crystals of graphene oxide. *Nat. Commun.* **7**, 1–12 (2016).
15. Goh, K. et al. All-carbon nanoarchitectures as high-performance separation membranes with superior stability. *Adv. Funct. Mater.* **25**, 7348–7359 (2015).
16. Perreault, F., Fonseca De Faria, A. & Elimelech, M. Environmental applications of graphene-based nanomaterials. *Chem. Soc. Rev.* **44**, 5861–5896 (2015).
17. Huang, L., Zhang, M., Li, C. & Shi, G. Graphene-based membranes for molecular separation. *J. Phys. Chem. Lett.* **6**, 2806–2815 (2015).
18. Abraham, J. et al. Tunable sieving of ions using graphene oxide membranes. *Nat. Nanotechnol.* **12**, 546–550 (2017).
19. Wang, Y., He, Z., Gupta, K. M., Shi, Q. & Lu, R. Molecular dynamics study on water desalination through functionalized nanoporous graphene. *Carbon* **116**, 120–127 (2017).
20. Jain, T. et al. Heterogeneous sub-continuum ionic transport in statistically isolated graphene nanopores. *Nat. Nanotechnol.* **10**, 1053–1057 (2015).
21. Surwade, S. P. et al. Water desalination using nanoporous single-layer graphene. *Nat. Nanotechnol.* **10**, 459–464 (2015).
22. O'Hern, S. C. et al. Selective ionic transport through tunable subnanometer pores in single-layer graphene membranes. *Nano Lett.* **14**, 1234–1241 (2014).
23. O'Hern, S. C. et al. Selective molecular transport through intrinsic defects in a single layer of CVD graphene. *ACS Nano* **6**, 10130–10138 (2012).
24. Koenig, S. P., Wang, L., Pellegrino, J. & Bunch, J. S. Selective molecular sieving through porous graphene. *Nat. Nanotechnol.* **7**, 728–732 (2012).

25. Wang, E. N. & Karnik, R. Graphene cleans up water. *Nat. Nanotechnol.* **7**, 552–554 (2012).
26. Cohen-Tanugi, D. & Grossman, J. C. Water desalination across nanoporous graphene. *Nano Lett.* **12**, 3602–3608 (2012).
27. Wang, Z. & Mi, B. Environmental applications of 2D molybdenum disulfide (MoS2) nanosheets. *Environ. Sci. Technol.* **51**, 8229–8244 (2017).
28. Wang, Z. et al. Understanding the aqueous stability and filtration capability of MoS2 membranes. *Nano Lett.* **17**, 7289–7298 (2017).
29. Abraham, J. et al. Tuneable sieving of ions using graphene oxide membranes. *Nat. Nanotechnol.* **12**, 546–550 (2017).
30. Li, H. et al. Ultrathin, molecular-sieving graphene oxide membranes for selective hydrogen separation. *Science* **342**, 95–98 (2013).
31. Kim, H. W. et al. Selective gas transport through few-layered graphene and graphene oxide membranes. *Science* **342**, 91–95 (2013).
32. Nair, R. R., Wu, H. A., Jayaram, P. N., Grigorieva, I. V. & Geim, A. K. Unimpeded permeation of water through helium-leak-tight graphene-based membranes. *Science* **335**, 442–444 (2012).
33. Homaeigohar, S. & Elbahri, M. Graphene membranes for water desalination. *NPG Asia Mater.* **9**, e427–e427 (2017).
34. Werber, J. R., Osuji, C. O. & Elimelech, M. Materials for next-generation desalination and water purification membranes. *Nat. Rev. Mater.* **1**, 1–15 (2016).
35. Bera, S. et al. 2D-nanofiller-based polymer nanocomposites for capacitive energy storage applications. *Small Sci.* **3**, 2300016 (2023).
36. Sonker, M. et al. Ammonia as an alternative fuel for vehicular applications: Paving the way for adsorbed ammonia and direct ammonia fuel cells. *J. Clean. Prod.* **376**, 133960 (2022).
37. Alkhouzaam, A. & Qiblawey, H. Functional GO-based membranes for water treatment and desalination: fabrication methods, performance and advantages. A review. *Chemosphere* **274**, 129853 (2021).
38. Yang, Q. et al. Ultrathin graphene-based membrane with precise molecular sieving and ultrafast solvent permeation. *Nat. Mater.* **16**, 1198–1202 (2017).
39. Ritt, C. L., Werber, J. R., Deshmukh, A. & Elimelech, M. Monte Carlo simulations of framework defects in layered two-dimensional nanomaterial desalination membranes: implications for permeability and selectivity. *Environ. Sci. Technol.* **53**, 6214–6224 (2019).
40. Zhang, W.-H. et al. Membrane preparation Graphene oxide membranes with stable porous structure for ultrafast water transport. *Nat. Nanotechnol.* **16**, 337–343 (2021).
41. Yeh, C. N., Raidongia, K., Shao, J., Yang, Q. H. & Huang, J. On the origin of the stability of graphene oxide membranes in water. *Nat. Chem.* **7**, 166–170 (2014).
42. Park, M. J. et al. Graphene oxide incorporated polysulfone substrate for the fabrication of flat-sheet thin-film composite forward osmosis membranes. *J. Memb. Sci.* **493**, 496–507 (2015).
43. Guo, J. et al. Ultra-permeable dual-mechanism-driven graphene oxide framework membranes for precision ion separations. *Angew. Chem. Int. Ed.* **62**, e202302931 (2023).
44. Park, S. et al. Graphene oxide papers modified by divalent ions—enhancing mechanical properties via chemical cross-linking. *ACS Nano* **2**, 572–578 (2008).
45. Sun, P., Wang, K. & Zhu, H. Recent developments in graphene-based membranes: structure, mass-transport mechanism and potential applications. *Adv. Mater.* **28**, 2287–2310 (2016).
46. Ali, A. et al. Graphene-based membranes for CO2 separation. *Mater. Sci. Energy Technol.* **2**, 83–88 (2019).
47. An, D., Yang, L., Wang, T.-J. & Liu, B. Separation performance of graphene oxide membrane in aqueous solution. *Ind. Eng. Chem. Res.* **17**, 4803–4810 (2016).
48. Kumar, Y. et al. Nanomaterials: stimulants for biofuels and renewables, yield and energy optimization. *Mater. Adv.* **2**, 5318–5343 (2021).
49. Zhu, L. et al. Graphene oxide composite membranes for water purification. *ACS Appl. Nano Mater.* **5**, 3643–3653 (2022).
50. Mi, B. Graphene oxide membranes for ionic and molecular sieving. *Science* **343**, 740–742 (2014).
51. Singh, M., Tiwary, S. K. & Karim, A. Sub-nano fillers for high-temperature storage. *Nat. Energy* **9**, 113–114 (2024).
52. Tiwary, S. K. et al. Self-cross-linking of MXene-intercalated graphene oxide membranes with antiswelling properties for dye and salt rejection. *ACS Environ. Au* **4**, 69–79 (2024).
53. Zhang, Y. & Chung, T. S. Graphene oxide membranes for nanofiltration. *Curr. Opin. Chem. Eng.* **16**, 9–15 (2017).
54. Nan, Q., Li, P. & Cao, B. Fabrication of positively charged nanofiltration membrane via the layer-by-layer assembly of graphene oxide and polyethylenimine for desalination. *Appl. Surf. Sci.* **387**, 521–528 (2016).
55. Lim, M. Y. et al. Cross-linked graphene oxide membrane having high ion selectivity and antibacterial activity prepared using tannic acid-functionalized graphene oxide and polyethyleneimine. *J. Memb. Sci.* **521**, 1–9 (2017).
56. Han, Y., Xu, Z. & Gao, C. Ultrathin graphene nanofiltration membrane for water purification. *Adv. Funct. Mater.* **23**, 3693–3700 (2013).
57. Wang, Z., Ma, C., Sinquefield, S. A., Shofner, M. L. & Nair, S. High-performance graphene oxide nanofiltration membranes for black liquor concentration. ACS Sustain. *Chem. Eng.* **7**, 14915–14923 (2019).
58. Istirokhatun, T. et al. Unveiling the impact of imidazole derivative with mechanistic insights into neutralize interfacial polymerized membranes for improved solute-solute selectivity. *Water Res.* **230**, 119567 (2023).
59. Irshad, M. S. et al. Highly charged solar evaporator toward sustainable energy transition for in-situ freshwater & power generation. *Chem. Eng. J.* **458**, 141431 (2023).
60. He, H. & Gao, C. General approach to individually dispersed, highly soluble, and conductive graphene nanosheets functionalized by nitrene chemistry. *Chem. Mater.* **22**, 5054–5064 (2010).
61. Xu, Z. & Gao, C. In situ polymerization approach to graphene-reinforced nylon-6 composites. *Macromolecules* **43**, 6716–6723 (2010).
62. Xu, Z. & Gao, C. Aqueous Liquid Crystals of Graphene Oxide. *ACS Nano* **5**, 2908–2915 (2011).
63. Peeters, J. M. M., Boom, J. P., Mulder, M. H. V. & Strathmann, H. Retention measurements of nanofiltration membranes with electrolyte solutions. *J. Memb. Sci.* **145**, 199–209 (1998).
64. Kieu, H. T., Zhou, K. & Law, A. W. K. Surface morphology effect on the evaporation of water on graphene oxide: a molecular dynamics study. *Appl. Surf. Sci.* **488**, 335–342 (2019).
65. Chowdury, M. S. K., Cho, Y. J., Park, S. B. & Park, Y. Review—functionalized graphene oxide membranes as electrolytes. *J. Electrochem. Soc.* **170**, 033503 (2023).
66. Pirillo, S., Pedroni, V., Rueda, E. & Ferreira, M. L. Elimination of dyes from aqueous solutions using iron oxides and chitosan as adsorbents: a comparative study. *Quim. Nova* **32**, 1239–1244 (2009).
67. Shalaby, S. M., Madkour, F. F., El-Kassas, H. Y., Mohamed, A. A. & Elgarahy, A. M. Green synthesis of recyclable iron oxide nanoparticles using Spirulina platensis microalgae for adsorptive removal of cationic and anionic dyes. *Environ. Sci. Pollut. Res.* **28**, 65549–65572 (2021).
68. Shreyash, N. et al. Green synthesis of nanoparticles and their biomedical applications: a review. *ACS Appl. Nano Mater.* **4**, 11428–11457 (2021).

69. Kang, Y., Jang, J., Lee, Y. & Kim, I. S. Dye adsorptive thin-film composite membrane with magnetite decorated sulfonated graphene oxide for efficient dye/salt mixture separation. *Desalination* **524**, 115462 (2022).
70. Xu, C., Cui, A., Xu, Y. & Fu, X. Graphene oxide-TiO2 composite filtration membranes and their potential application for water purification. *Carbon* **62**, 465–471 (2013).
71. Bajpai, S., Shreyash, N., Sonker, M., Tiwary, S. K. & Biswas, S. Investigation of SiO_2 nanoparticle retention in flow channels, its remediation using surfactants and relevance of artificial intelligence in the future. *Chemistry* **3**, 1371–1380 (2021).
72. Bajpai, S. et al. Recent advances in nanoparticle-based cancer treatment: a review. *ACS Appl. Nano Mater.* **4**, 6441–6470 (2021).
73. Shreyash, N., Sonker, M., Bajpai, S. & Tiwary, S. K. Review of the mechanism of nanocarriers and technological developments in the field of nanoparticles for applications in cancer theragnostics. *ACS Appl. Bio Mater.* **4**, 2307–2334 (2021).
74. Sonker, M. et al. Review of recent advances and their improvement in the effectiveness of hydrogel-based targeted drug delivery: a hope for treating cancer. *ACS Appl. Bio Mater.* **4**, 8080–8109 (2021).
75. Han, Y., Jiang, Y. & Gao, C. High-flux graphene oxide nanofiltration membrane intercalated by carbon nanotubes. *ACS Appl. Mater. Interfaces* **7**, 30 (2015).
76. Ge, R., Huo, T., Gao, Z., Li, J. & Zhan, X. GO-based membranes for desalination. *Membranes* **13**, 220 (2023).
77. Dahanayaka, M., Liu, B., Srikanth, N. & Zhou, K. Ionised graphene oxide membranes for seawater desalination. *Desalination* **496**, 114637 (2020).
78. Li, Z., Han, Q. & Qiu, Y. Field-enhanced water transport in sub-nanometer graphene nanopores. *Desalination* **528**, 115610 (2022).
79. Huang, H. H., Joshi, R. K., De Silva, K. K. H., Badam, R. & Yoshimura, M. Fabrication of reduced graphene oxide membranes for water desalination. *J. Memb. Sci.* **572**, 12–19 (2019).
80. Tang, B. et al. Are vacuum-filtrated reduced graphene oxide membranes symmetric? *Nanoscale* **8**, 1108–1116 (2015).
81. Chen, Z. et al. Electrically controlled thermal radiation from reduced graphene oxide membranes. *ACS Appl. Mater. Interfaces* **13**, 27278–27283 (2021).
82. Pei, J., Zhang, X., Huang, L., Jiang, H. & Hu, X. Fabrication of reduced graphene oxide membranes for highly efficient water desalination. *RSC Adv.* **6**, 101948–101952 (2016).
83. An, Y. C. et al. A critical review on graphene oxide membrane for industrial wastewater treatment. *Environ. Res.* **223**, 115409 (2023).
84. Chen, C. et al. Understanding the effect of hydroxyl/epoxy group on water desalination through lamellar graphene oxide membranes via molecular dynamics simulation. *Desalination* **491**, 114560 (2020).
85. Gao, X., Jang, J. & Nagase, S. Hydrazine and thermal reduction of graphene oxide: reaction mechanisms, product structures, and reaction design. *J. Phys. Chem. C* **114**, 832–842 (2010).
86. Liu, H., Wang, H. & Zhang, X. Facile fabrication of freestanding ultrathin reduced graphene oxide membranes for water purification. *Adv. Mater.* **27**, 249–254 (2015).
87. Qi, B. et al. Strict molecular sieving over electrodeposited 2D-interspacing-narrowed graphene oxide membranes. *Nat. Commun.* **8**, 1–10 (2017).
88. Lin, L. C. & Grossman, J. C. Atomistic understandings of reduced graphene oxide as an ultrathin-film nanoporous membrane for separations. *Nat. Commun.* **6**, 1–7 (2015).
89. Zhou, D., Cheng, Q. Y. & Han, B. H. Solvothermal synthesis of homogeneous graphene dispersion with high concentration. *Carbon* **49**, 3920–3927 (2011).
90. Novoselov, K. S. et al. Electric field in atomically thin carbon films. *Science* **306**, 666–669 (2004).
91. López, V. et al. Chemical vapor deposition repair of graphene oxide: a route to highly-conductive graphene monolayers. *Adv. Mater.* **21**, 4683–4686 (2009).
92. Some, S. et al. High-quality reduced graphene oxide by a dual-function chemical reduction and healing process. *Sci. Rep.* **3**, 1–5 (2013).
93. Zhang, W. et al. General synthesis of ultrafine metal oxide/reduced graphene oxide nanocomposites for ultrahigh-flux nanofiltration membrane. *Nat. Commun.* **13**, 1–10 (2022).
94. Han, T. H., Huang, Y. K., Tan, A. T. L., Dravid, V. P. & Huang, J. Steam etched porous graphene oxide network for chemical sensing. *J. Am. Chem. Soc.* **133**, 15264–15267 (2011).
95. Zhou, D., Cui, Y., Xiao, P. W., Jiang, M. Y. & Han, B. H. A general and scalable synthesis approach to porous graphene. *Nat. Commun.* **5**, 1–7 (2014).
96. Berger, C. et al. Ultrathin epitaxial graphite: 2D electron gas properties and a route toward graphene-based nanoelectronics. *J. Phys. Chem. B* **108**, 19912–19916 (2004).
97. Kim, S. et al. Room-temperature metastability of multilayer graphene oxide films. *Nat. Mater.* **11**, 544–549 (2012).
98. Woo Kim, D. et al. Revealing the role of oxygen debris and functional groups on the water flux and molecular separation of graphene oxide membrane: a combined experimental and theoretical study. *J. Phys. Chem. C* **122** (2018).
99. Wang, Z. et al. The stability of a graphene oxide (GO) nanofiltration (NF) membrane in an aqueous environment: progress and challenges. *Mater. Adv.* **1**, 554–568 (2020).
100. Zhao, Z., Ni, S., Su, X., Gao, Y. & Sun, X. Thermally reduced graphene oxide membrane with ultrahigh rejection of metal ions' separation from water. *ACS Sustain Chem. Eng.* **7**, 14874–14882 (2019).
101. Gao, Y. et al. The effect of interlayer adhesion on the mechanical behaviors of macroscopic graphene oxide papers. *ACS Nano* **5**, 2134–2141 (2011).
102. Koltonow, A. R., Luo, C., Luo, J. & Huang, J. Graphene oxide sheets in solvents: to crumple or not to crumple? *ACS Omega* **2**, 8005–8009 (2017).
103. Qian, X., Li, N., Wang, Q. & Ji, S. Chitosan/graphene oxide mixed matrix membrane with enhanced water permeability for high-salinity water desalination by pervaporation. *Desalination* **438**, 83–96 (2018).
104. Nie, L. et al. Realizing small-flake graphene oxide membranes for ultrafast size-dependent organic solvent nanofiltration. *Sci. Adv.* **6**, eaaz9184 (2020).
105. Jang, J. H., Woo, J. Y., Lee, J. & Han, C. S. Ambivalent effect of thermal reduction in mass rejection through graphene oxide membrane. *Environ. Sci. Technol.* **50**, 10024–10030 (2016).
106. Li, W., Wu, W. & Li, Z. Controlling interlayer spacing of graphene oxide membranes by external pressure regulation. *ACS Nano* **12**, 9309–9317 (2018).
107. Zhang, M. et al. Molecular bridges stabilize graphene oxide membranes in water. *Angew. Chem. Int. Ed.* **59**, 1689–1695 (2020).
108. Chen, L. et al. Ion sieving in graphene oxide membranes via cationic control of interlayer spacing. *Nature* **550**, 380–383 (2017).
109. Wilson, N. R. et al. Graphene oxide: structural analysis and application as a highly transparent support for electron microscopy. *ACS Nano* **3**, 2547–2556 (2009).
110. Loh, K. P., Bao, Q., Eda, G. & Chhowalla, M. Graphene oxide as a chemically tunable platform for optical applications. *Nat. Chem.* **2**, 1015–1024 (2010).
111. Zhang, Y., Zhang, S. & Chung, T. S. Nanometric graphene oxide framework membranes with enhanced heavy metal removal via nanofiltration. *Environ. Sci. Technol.* **49**, 10235–10242 (2015).
112. Sun, P. et al. Highly efficient quasi-static water desalination using monolayer graphene oxide/titania hybrid laminates. *NPG Asia Mater.* **7**, e162–e162 (2015).

113. Debnath, S., Tiwary, S. K. & Ojha, U. Dynamic carboxylate linkage based reprocessable and self-healable segmented polyurethane vitrimers displaying creep resistance behavior and triple shape memory ability. *ACS Appl Polym. Mater.* **3**, 2166–2177 (2021).
114. Lai, G. S. et al. Graphene oxide incorporated thin film nanocomposite nanofiltration membrane for enhanced salt removal performance. *Desalination* **387**, 14–24 (2016).
115. Xu, Y. et al. Chemically converted graphene-induced molecular flattening of 5,10,15,20-tetrakis(1-methyl-4-pyridinio)porphyrin and its application for optical detection of cadmium(II) ions. *J. Am. Chem. Soc.* **131**, 13490–13497 (2009).
116. Sun, L., He, X. & Lu, J. Super square carbon nanotube network: a new promising water desalination membrane. *npj Comput. Mater.* **2**, 1–7 (2016).
117. Dreyer, D. R., Park, S., Bielawski, C. W. & Ruoff, R. S. The chemistry of graphene oxide. *Chem. Soc. Rev.* **39**, 228–240 (2009).
118. Yu, J., He, Y., Wang, Y., Zhang, L. & Hou, R. Graphene oxide nanofiltration membrane for efficient dyes separation by hexagonal boron nitride nanosheets intercalation and polyethyleneimine surface modification. *Colloids Surf. A Physicochem. Eng. Asp.* **656**, 130367 (2023).
119. Morelos-Gomez, A. et al. Effective NaCl and dye rejection of hybrid graphene oxide/graphene layered membranes. *Nat. Nanotechnol.* **12**, 1083–1088 (2017).
120. Wang, Z. et al. Graphene oxide nanofiltration membranes for desalination under realistic conditions. *Nat. Sustain.* **4**, 402–408 (2021).
121. Sun, J., Iakunkov, A., Rebrikova, A. T. & Talyzin, A. V. Exactly matched pore size for the intercalation of electrolyte ions determined using the tunable swelling of graphite oxide in supercapacitor electrodes. *Nanoscale* **10**, 21386–21395 (2018).
122. Zheng, S., Tu, Q., Wang, M., Urban, J. J. & Mi, B. Correlating interlayer spacing and separation capability of graphene oxide membranes in organic solvents. *ACS Nano* **14**, 6013–6023 (2020).
123. Nordenström, A. et al. Intercalation of dyes in graphene oxide thin films and membranes. *J. Phys. Chem. C.* **125**, 6885 (2021).
124. Xu, X. L. et al. Graphene oxide nanofiltration membranes stabilized by cationic porphyrin for high salt rejection. *ACS Appl Mater. Interfaces* **8**, 12588–12593 (2016).
125. Han, J. L. et al. Borate inorganic cross-linked durable graphene oxide membrane preparation and membrane fouling control. *Environ. Sci. Technol.* **53**, 1501–1508 (2019).
126. Yan, X. et al. D-spacing controllable GO membrane intercalated by sodium tetraborate pentahydrate for dye contamination wastewater treatment. *J. Hazard Mater.* **422**, 126939 (2022).
127. Zhang, M. et al. Controllable ion transport by surface-charged graphene oxide membrane. *Nat. Commun.* **10**, 1–8 (2019).
128. Geise, G. M., Park, H. B., Sagle, A. C., Freeman, B. D. & McGrath, J. E. Water permeability and water/salt selectivity tradeoff in polymers for desalination. *J. Memb. Sci.* **369**, 130–138 (2011).
129. Werber, J. R., Deshmukh, A. & Elimelech, M. The critical need for increased selectivity, not increased water permeability, for desalination membranes. *Environ. Sci. Technol. Lett.* **3**, 112–120 (2016).
130. Zhang, M. et al. Nanoparticles@rGO membrane enabling highly enhanced water permeability and structural stability with preserved selectivity. *AIChE J.* **63**, 5054–5063 (2017).
131. Yang, Y. et al. Large-area graphene-nanomesh/ carbon-nanotube hybrid membranes for ionic and molecular nanofiltration. *Science (1979)* **364**, 1057–1062 (2019).
132. Nguyen, C. T. & Beskok, A. Charged nanoporous graphene membranes for water desalination. *Phys. Chem. Chem. Phys.* **21**, 9483–9494 (2019).
133. Zhang, W. H. et al. Graphene oxide membranes with stable porous structure for ultrafast water transport. *Nat. Nanotechnol.* **16**, 337–343 (2021).
134. Zhang, Z., Li, S., Mi, B., Wang, J. & Ding, J. Surface slip on rotating graphene membrane enables the temporal selectivity that breaks the permeability-selectivity trade-off. *Sci. Adv.* **6**, eaba9471 (2020).
135. Shi, E. et al. Carbon nanotube network embroidered graphene films for monolithic all-carbon electronics. *Adv. Mater.* **27**, 682–688 (2015).
136. Nielsen, F., Boissonnat, J.-D. & Nock, R. Bregman Voronoi diagrams: properties, algorithms and applications. *Discret. Comput Geom.* **44**, 281–307 (2007).
137. Nie, L. et al. Hyperlooping carbon nanotube-graphene oxide nanoarchitectonics as membranes for ultrafast organic solvent nanofiltration. *ACS Mater. Lett.* **5**, 357–369 (2023).
138. Tang, Y. J., Xu, Z. L., Xue, S. M., Wei, Y. M. & Yang, H. A chlorine-tolerant nanofiltration membrane prepared by the mixed diamine monomers of PIP and BHTTM. *J. Memb. Sci.* **498**, 374–384 (2016).
139. Fan, X., Liu, Y. & Quan, X. A novel reduced graphene oxide/carbon nanotube hollow fiber membrane with high forward osmosis performance. *Desalination* **451**, 117–124 (2018).
140. Lazarenko, N. S., Golovakhin, V. V., Shestakov, A. A., Lapekin, N. I. & Bannov, A. G. Recent advances on membranes for water purification based on carbon nanomaterials. *Membranes* **12**, 915 (2022).
141. Zhang, Z. et al. Theory and simulation developments of confined mass transport through graphene-based separation membranes. *Phys. Chem. Chem. Phys.* **22**, 6032–6057 (2020).
142. Sun, P. et al. Selective ion penetration of graphene oxide membranes. *ACS Nano* **7**, 428–437 (2013).
143. Castelletto, S. & Boretti, A. Advantages, limitations, and future suggestions in studying graphene-based desalination membranes. *RSC Adv.* **11**, 7981–8002 (2021).
144. Boukhvalov, D. W., Katsnelson, M. I. & Son, Y. W. Origin of anomalous water permeation through graphene oxide membrane. *Nano Lett.* **13**, 3930–3935 (2013).
145. Vatanpour, V. et al. TiO2 embedded mixed matrix PES nanocomposite membranes: Influence of different sizes and types of nanoparticles on antifouling and performance. *Desalination* **292**, 19–29 (2012).
146. Shi, X., Tal, G., Hankins, N. P. & Gitis, V. Fouling and cleaning of ultrafiltration membranes: a review. *J. Water Process Eng.* **1**, 121–138 (2014).
147. Amirilargani, M., Sabetghadam, A. & Mohammadi, T. Polyethersulfone/polyacrylonitrile blend ultrafiltration membranes with different molecular weight of polyethylene glycol: preparation, morphology and antifouling properties. *Polym. Adv. Technol.* **23**, 398–407 (2012).
148. Boretti, A. et al. Outlook for graphene-based desalination membranes. *npj Clean Water* **1**, 5 (2018).
149. Thebo, K. H. et al. Highly stable graphene-oxide-based membranes with superior permeability. *Nat. Commun.* **9**, 1–8 (2018).
150. Zhou, S. et al. Self-cleaning loose nanofiltration membranes enabled by photocatalytic Cu-triazolate MOFs for dye/salt separation. *J. Memb. Sci.* **623**, 119058 (2021).
151. Lin, H., Mehra, N., Li, Y. & Zhu, J. Graphite oxide/boron nitride hybrid membranes: the role of cross-plane laminar bonding for a durable membrane with large water flux and high rejection rate. *J. Membr. Sci.* **593**, 117401 (2019).
152. Dong, L. et al. NH2-Fe3O4-regulated graphene oxide membranes with well-defined laminar nanochannels for desalination of dye solutions. *Desalination* **476**, 114227 (2020).
153. Wei, Y., Zhu, Y. & Jiang, Y. Photocatalytic self-cleaning carbon nitride nanotube intercalated reduced graphene oxide membranes for enhanced water purification. *Chem. Eng. J.* **356**, 915–925 (2019).
154. Zhang, P. et al. Novel “loose” GO/MoS2 composites membranes with enhanced permeability for effective salts and dyes rejection at low pressure. *J. Memb. Sci.* **574**, 112–123 (2019).

155. Kang, D., Shao, H., Chen, G., Dong, X. & Qin, S. Fabrication of highly permeable PVDF loose nanofiltration composite membranes for the effective separation of dye/salt mixtures. *J. Membr. Sci.* **621**, 118951 (2021).
156. Safarpour, M., Khataee, A. & Vatanpour, V. Preparation of a novel polyvinylidene fluoride (PVDF) ultrafiltration membrane modified with reduced graphene oxide/titanium dioxide (TiO2) nanocomposite with enhanced hydrophilicity and antifouling properties. *Ind. Eng. Chem. Res* **53**, 13370–13382 (2014).
157. Chen, X., Qiu, M., Ding, H., Fu, K. & Fan, Y. A reduced graphene oxide nanofiltration membrane intercalated by well-dispersed carbon nanotubes for drinking water purification. *Nanoscale* **8**, 5696–5705 (2016).
158. Gao, S. J., Qin, H., Liu, P. & Jin, J. SWCNT-intercalated GO ultrathin films for ultrafast separation of molecules. *J. Mater. Chem. A Mater.* **3**, 6649–6654 (2015).
159. Yang, E. et al. Enhanced desalination performance of forward osmosis membranes based on reduced graphene oxide laminates coated with hydrophilic polydopamine. *Carbon* **117**, 293–300 (2017).
160. Zhao, C., Xu, X., Chen, J. & Yang, F. Effect of graphene oxide concentration on the morphologies and antifouling properties of PVDF ultrafiltration membranes. *J. Environ. Chem. Eng.* **1**, 349–354 (2013).
161. Sun, J. et al. Tailoring the microstructure of poly(vinyl alcohol)-intercalated graphene oxide membranes for enhanced desalination performance of high-salinity water by pervaporation. *J. Membr. Sci.* **599**, 117838 (2020).
162. Xue, S. M., Ji, C. H., Xu, Z. L., Tang, Y. J. & Li, R. H. Chlorine resistant TFN nanofiltration membrane incorporated with octadecylamine-grafted GO and fluorine-containing monomer. *J. Membr. Sci.* **545**, 185–195 (2018).
163. Bhadra, M., Rosy, S. & Mitra, S. Desalination across a graphene oxide membrane via direct contact membrane distillation. *Desalination* **378**, 37–43 (2016).
164. Hussain Thebo, K. et al. Highly stable graphene-oxide-based membranes with superior permeability. *Nat. Commun.* **9**, 1486 (2018).
165. Liu, Y. et al. A high stability GO nanofiltration membrane preparation by co-deposition and crosslinking polydopamine for rejecting dyes. *Water Sci. Technol.* **85**, 1783–1799 (2022).
166. Mao, L. et al. Stiffening of graphene oxide films by soft porous sheets. *Nat. Commun.* **10**, 1–7 (2019).

Acknowledgements

The authors acknowledge funding from NSF DMR#1900692, ACS PRF#66838-ND7, WELCH#E-2105-20220331, and WELCH#V-E-0003-20230731 grants for their generous support of our work.

Author contributions

Credit: Saurabh Kr Tiwary: conceptualization, investigation, data curation, project administration, formal analysis, writing; Maninderjeet Singh: investigation, resources, validation, writing-review & editing; Shubham Vasant Chavan: validation, visualization, writing-original draft; Alamgir Karim: supervision, visualization, writing-review & editing.

Competing interests

The authors declare no competing interests.

Additional information

Correspondence and requests for materials should be addressed to Alamgir Karim.